








Article

A Method for Assessment of Power Consumption Change in Distribution Grid Branch After Consumer Load Change

Marius Saunoris ^{1,*}, Julius Šaltanis ¹, Robertas Lukočius ¹, Vytautas Daunoras ¹, Kasparas Zulonas ¹, Evaldas Vaičiukynas ^{2,*} and Žilvinas Nakutis ¹

¹ Faculty of Electrical and Electronics Engineering, Kaunas University of Technology, LT-51368 Kaunas, Lithuania; julius.saltanis@ktu.lt (J.Š.); robertas.lukocius@ktu.lt (R.L.); vytautas.daunoras@ktu.lt (V.D.); kasparas.zulonas@ktu.lt (K.Z.); zilvinas.nakutis@ktu.lt (Ž.N.)
² Faculty of Information Engineering, Kaunas University of Technology, LT-51368 Kaunas, Lithuania
* Correspondence: marius.saunoris@ktu.lt (M.S.); evaldas.vaiciukynas@ktu.lt (E.V.)

Abstract

This research targets prediction of power consumption change (PCC) in the branch of electrical distribution grid between a sum meter and consumer meter in response to consumer load change. The problem is relevant for power preservation law-based event-driven methods aiming for detection of anomalies like meter errors, electricity thefts, etc. The PCC in the branch is due to the change of technical (wiring) losses as well as change of power consumption of loads connected to the same distribution branch. Using synthesized dataset set a data-driven model is built to predict PCC in the branch. Model performance is assessed using root mean squared error (RMSE), mean absolute, and mean relative error, together with their standard deviations. The preliminary experimental verification using a test bed confirmed the potential of the method. The accuracy of the PCC in the branch prediction is influenced by the systematic error of the meters. Therefore, the error of the consumer meter and the PCC in the branch cannot be evaluated separately. It was observed that the absolute error of the estimate of power measurement gain error was observed to be within $\pm 0.3\%$ and the relative error of PCC in the branch prediction was within $\pm 10\%$.

Keywords: power measurement; power distribution network; power loss; meter error



Academic Editors: Ningning Ma and Lei Chen

Received: 16 June 2025

Revised: 22 July 2025

Accepted: 23 July 2025

Published: 25 July 2025

Citation: Saunoris, M.; Šaltanis, J.; Lukočius, R.; Daunoras, V.; Zulonas, K.; Vaičiukynas, E.; Nakutis, Ž. A Method for Assessment of Power Consumption Change in Distribution Grid Branch After Consumer Load Change. *Appl. Sci.* **2025**, *15*, 8299. <https://doi.org/10.3390/app15158299>

Copyright: © 2025 by the authors. Licensee MDPI, Basel, Switzerland. This article is an open access article distributed under the terms and conditions of the Creative Commons Attribution (CC BY) license (<https://creativecommons.org/licenses/by/4.0/>).

1. Introduction

The smart nature of modern metering devices, together with Advanced Metering Infrastructure (AMI), greatly extends the scope of their functionality [1–4]. A smart meter is electrical energy revenue electronic meter equipped with diverse communication capabilities. Additional features such as high-resolution data acquisition, on-device storage, bidirectional communication, time synchronization, real-time data processing, and event detection enable smart meters to support applications far beyond those of conventional electromechanical meters [5–9]. Smart electric energy meters can measure and transmit values of current, voltage, active and reactive power, and power factor at sufficiently high time resolution [10,11]. These data streams enable continuous monitoring of grid conditions and facilitate the detection of anomalies, such as meter faults [12,13], non-technical energy losses [14–16], atypical consumption patterns, infrastructure degradation, power interruptions, or equipment malfunctions [17–19].

To fully leverage these functionalities, advanced methods for data analysis and interpretation must be developed. This need has attracted substantial attention in recent

research. Most anomaly detection methods proposed for smart meter data are grounded in statistical analysis and machine learning techniques. The employed models include linear regression frameworks (e.g., least squares), support vector machines, least squares support vector regression, Gaussian process models, deep neural networks, unsupervised clustering methods, decision tree ensembles, regularization-based methods, and various optimization algorithms [20–27].

Revenue energy meters fall under the scope of legal metrology. Manufactured meters undergo metrological verification for compliance with the requirements of standards like IEC 62053-21 or EN 50470-3. Country-dependent regulations define the energy meter's period of the first reverification, which typically is in the range of 6 to 12 years [28]. It is expected that before the expiration of the verification period meter's measuring error does not exceed the limits described in the corresponding standard, for example, 1% of energy measurement for the class 1 meters. However, due to the ageing phenomenon, quality of electronics assembly, impact of harsh environmental conditions, malicious acts, etc., may cause metering error to exceed allowed limits. In this case, the larger the meter error, the higher the economic losses energy provider or consumer will experience. Therefore, it is important to detect meters that do not comply with the standard requirements. In some cases, consumers may complain or utilities detect unexpected behavior of meters, also a meter may report its malfunctioning mode if self-diagnostics features are implemented. In all cases, the meter is removed from service and replaced with the new meter. In practice, error correction is never applied for the revenue meters that are found to exceed errors defined by the standard. Therefore, the key requirement in order to minimize economic losses or errors of power consumption forecasts is to detect the malfunctioning meter as fast as possible. Consumer complaints can be incorrect (the meter is found to operate properly), and sending utility personnel to perform on-site verification or deliver a meter for metrological verification in-laboratory is a costly procedure. Therefore, the reliability of detection of a suspected meter is of utmost importance. Remote meter error detection methods are aimed at identifying the suspected meters that have to be replaced with new metrologically certified meters according to the internal procedures of the electricity providing utility. Quantification of the impact of metering errors could be performed to determine economic losses due to incorrect metering. Some considerations on this issue were presented in our previous articles [13]. Typically, if meters are compliant with the corresponding standards, the impact of systematic errors (within allowed limits) and economic losses to consumers and energy providers are expected to be equally distributed, and no actions are applied to correct meters reported consumption readings.

Many of the suggested methods are based on the analysis of long-term time series of power consumption and other electrical quantity data [29–33]. This strategy involves tracking energy usage patterns over time and comparing them to expected baseline behavior [29,34]. Another widely applied strategy is based on power balance analysis, which requires aggregating measurements from a sum (total) meter and comparing them with the cumulative readings of all downstream submeters in the power distribution network [20,21,35,36]. A sum meter is a smart meter that is installed at the beginning of the energy distribution branch and monitors total consumption of loads connected to the same branch and losses in the distribution electrical cables. The reliability and applicability of such methods diminish in practical deployment scenarios where smart metering coverage is incomplete or partially implemented.

In our previous work [37], we proposed an alternative method for detection of anomalies in smart metering data, which is based on the observation of discrete power events, sudden changes in load resulting from consumer activity, such as switching appliances on or off. This approach involves the joint analysis of power, current and voltage mea-

measurements obtained simultaneously from a sum meter and a meter under test (MUT), both before and after such power events. The sum meter serves as a reference instrument which readings are trusted both at the period of training of models necessary for the implementation and monitoring period. A power event (or power step), is defined as a distinct transition in energy demand at a specific time. This direct comparative method between meters eliminates the need for exhaustive submetering of all individual loads beneath the sum meter, a requirement that constrains many conventional techniques. Our method is based on evaluating the active power balance associated with a power consumption change (PCC) during a power step. The key equation is expressed as follows:

$$dP_s = dP_c + dP_n + dP_A, \quad (1)$$

where dP_s is an active PCC at the sum meter installation point, dP_c is active PCC of the load located under the consumer MUT, dP_A is PCC associated with a presence of the anomaly and dP_n is the change of active power consumption in the distribution branch. As presented in (2), PCC in the distribution branch in response to the consumer load consumption change (power step) is a superposition of (1) change of energy transfer losses in the distribution branch between sum meter and consumer meter, and (2) change of power consumption by other loads connected to the same distribution branch.

$$dP_n = dP_w + dP_{nL}. \quad (2)$$

The reason for the dP_w is power losses in energy delivery cables, and the reason for the dP_{nL} is power consumption change due to voltage change caused by the change of the consumer load behind MUT. This decomposition facilitates building a prediction model as derived later, but its constituent parts dP_w and dP_{nL} are not measured separately in a real distribution network.

The change of power associated with technical losses dP_w in the section of the distribution network or installation wiring between sum meter and consumer MUT, can be calculated—provided the impedances of each segment and the respective current readings are known—using the expression

$$dP_w = \sum_{i=1}^N I_{wi2}^2 R_{wi} - \sum_{i=1}^N I_{wi1}^2 R_{wi}, \quad (3)$$

where I_{wi1} and I_{wi2} are the currents in the i th line (cable) segment, before and after the power step dP_c , respectively, R_{wi} is wire resistance of the i th line's (cable's) segment, N is number of line segments between consecutive load connection points in the grid.

Numerous methods have been proposed for estimate technical losses, which depend on available information, network topology, and voltage levels. For low-voltage distribution networks, accurate loss estimation becomes particularly challenging due to the large number of elements and insufficient operational data [38].

One of the most straightforward approaches to estimating losses in low-voltage grids involves comparing the total energy supplied and consumed [39–42]. However, this method cannot distinguish between technical and non-technical losses [40,43], making it unsuitable for anomaly detection. Moreover, it requires synchronized or time-aggregated readings from both the entry-point meter and all load meters downstream. In real-world settings, data from some consumers is often unavailable due to non-telemetered loads [44,45]. Sometimes data from users is also unavailable due to disaster. Then, a load restoration method is required. This method must also consider losses (disconnections). In [46], an asynchronous

decentralized load restoration method of the resilient electricity-transportation network considering building and electric bus was presented.

Several methods have been developed to estimate missing data from non-telemetered customers or uncertain smart meter readings. For instance, Velasco J. A. and others [44] propose a top-down approach using intra-hour demand profiles generated via a Markov process, while Li Z. and others [47] suggest a Dirichlet-sampled Gaussian mixture model. However, such synthetic profiles are insufficient to accurately estimate instantaneous power loss changes triggered by specific load events, which is critical for our method.

Another class of techniques estimates technical losses via analytical approximations using parameters such as load form factor, loss factor, energy loss ratios, and empirically derived coefficients [38–40,48–55]. While these models are computationally simple and only require loading data at the entry point, their estimates are based on peak demand and general load profiles, lacking real-time responsiveness [48]. Thus, they are valuable for planning and optimization [40,56,57] but inadequate for event-based loss estimation in consumer delivery branches.

Benchmarking methods approximate a target network by matching it to a representative circuit from a library of benchmark models [40,45,58]. Selection is based on similarity between various features such as feeder length, number of branches, and customer density [45,59]. These techniques employ machine learning or statistical clustering to build and navigate the benchmark library [48]. However, the selected benchmark is an approximation rather than an exact match, which limits its usefulness for precise loss estimation [39].

Power flow analysis is a widely accepted method for estimating power losses [39,43,60–63]. It can yield high precision [60] but requires complete knowledge of network parameters and all load data. Since our method relies only on readings from the sum meter and the consumer MUT and assumes no access to detailed grid topology or wiring specifications, neither power flow analysis nor analytical loss estimation via (3) is applicable for our purposes.

In [64], a fundamentally different technique is proposed based on Newton’s law of cooling, which utilizes non-electrical parameters such as conductor and ambient temperatures. Although rooted in heat transfer physics, this method requires additional instrumentation (e.g., temperature sensors and data transmission systems) and suffers from slow thermal response and low sensitivity to small power changes, making it incompatible with our anomaly detection objectives.

The PCC component associated with changes in grid loads dP_{nL} , caused by a consumer load event dP_c , arises due to voltage fluctuations across the network. These voltage changes stem from altered current flows and the corresponding shifts in voltage drops. The response of each load to voltage variation—and hence its individual PCC component, dP_i —depends on the electrical nature of the load (e.g., constant power, constant current, or constant impedance), or their ZIP model composition [62,65].

If the ZIP model parameters of all loads and their voltage readings are known, then dP_{nL} can be calculated analytically:

$$dP_{nL} = \sum_{i=1}^M P_{iN} \left(a_i + b_i \frac{V_{i2}}{V_N} + c_i \left(\frac{V_{i2}}{V_N} \right)^2 \right) - \sum_{i=1}^M P_{iN} \left(a_i + b_i \frac{V_{i1}}{V_N} + c_i \left(\frac{V_{i1}}{V_N} \right)^2 \right), \quad (4)$$

where P_{iN} is power consumed by i th load when its voltage equals to the nominal $V_i = V_N$, a_i , b_i , c_i are the coefficients representing the constant power, constant current, and constant impedance components of the ZIP load model, V_{i2} and V_{i1} are actual voltages of the nodes where i th load is connected, correspondingly, before power step dP_c and after it. However, in practical deployments, voltage readings are often unavailable due to partial smart meter coverage, and the ZIP model parameters of connected loads are generally unknown. This significantly limits the applicability of (4) to real-world grid monitoring.

For the identification of the anomaly $dP_A \neq 0$, the suggested method requires evaluation of the PCC component dP_n (1). As discussed, it could not be done by applying previously presented analytical approaches (3) and (4) as the method relies just on data provided by sum meter and consumer smart meter, and the currents, voltages and powers of other consumers' loads connected to the distribution branch monitored by the sum meter (except the one monitored by consumer MUT) are unknown. It also cannot be obtained directly from the data acquired by sum meter and MUT if PCC component associated with the anomaly dP_A is suspected to be non-zero (1). However, dP_n could be predicted by applying statistical analysis or machine learning (ML) methods. Therefore, the aim of this work is to propose and verify a method for the prediction of PCC in distribution branch, which is caused by the PCC at consumer site using readings (powers, voltages, currents) acquired by sum meter and meter under test. It is assumed that readings of the other consumer loads, connected to the distribution branch, are unavailable because of partial smart metering deployment. If consumer MUT readings are used as input predictors (variables) for input of the prediction model, then its systematic error will influence the target output errors. Therefore, PCC and consumer MUT errors cannot be evaluated separately and become a common consumer MUT error and PCC assessment.

The main contribution of the paper is a method for estimation of PCC in the distribution branch in response to consumer load change. As can be seen from the survey of related literature (Table 1) of loss assessment techniques any method suitable for this specific task was not published earlier. A technique suggested in this paper targets improvement of event-driven accuracy of the method of remote meter error detection published in our earlier publication [37] by means of predicting PCC in the distribution branch between sum meter and consumer MUT. As the technique of remote error detection [37] relies on power preservation law, its accuracy improvement is achievable due to prediction of losses change in the distribution branch, and other same branch-connected loads' power consumption, which are members of the power balance equation.

Table 1. Summary of the methods for LV grid losses assessment.

References	Measure of Losses	The Main Principle	Required Data, Models and/or Tools	Limitations
[41,42,44,47]	Difference between input and output powers (energies).	Based on power (energy) balance.	Power readings at the entry point and of all loads (or output). Prediction model for the unmonitored loads for the partial smart-meter deployment cases.	All loads must be monitored by the smart meters; this does not provide an opportunity to discern technical and non-technical losses. Approximate data of the non-monitored loads for the partial smart-meter deployment cases.
[39,40,49–52]	Load loss factor, load factor, empirical coefficients.	Based on analytical approximations.	Power (energy) or current data at the entry point and factors, coefficients analytical approximations.	Are based on rougher approximations and provide rough losses estimates. Do not provide real-time information.
[45,58,59]	Losses of the equivalent circuit.	Based on reference grid models.	Power readings at the entry point. Set of benchmark circuits or approximations. Model, assessing similarities of the circuits.	Provides approximate estimates which accuracy depends on similarity of the analyzed network and its approximation.
[39,43,60,61]	The losses estimates based on Power-flow calculation.	Based on power-flow analysis.	Detailed technical specifications of the network. The data about all loads in the network, power flow analysis software.	Requires complete data about the network (technical specifications) and all loads.
[64]	Temperatures of the conductors and environment.	Based on Newton's Law of Cooling.	Data of conductors and environment temperatures, data gathering, transmission equipment, interpretation algorithms.	The inertia of the thermal processes and low sensitivity to the small power steps. Requires additional sensors, interpretation algorithms.

2. Materials and Methods

2.1. Equivalent Circuit of the Distribution Grid Branch

An equivalent circuit of a single-line diagram of the distribution grid branch representation for the verification of the power change prediction during the consumer power step by the suggested method is presented in Figure 1. The scheme mimics a common radial LV power supply path from a sum meter (SM) to a remote consumer meter under test (consumer MUT). Consequently, connected consumer loads $i = 1, N$ as well as the consumer MUT are separated by the line segments, which are represented by resistances in the circuit.

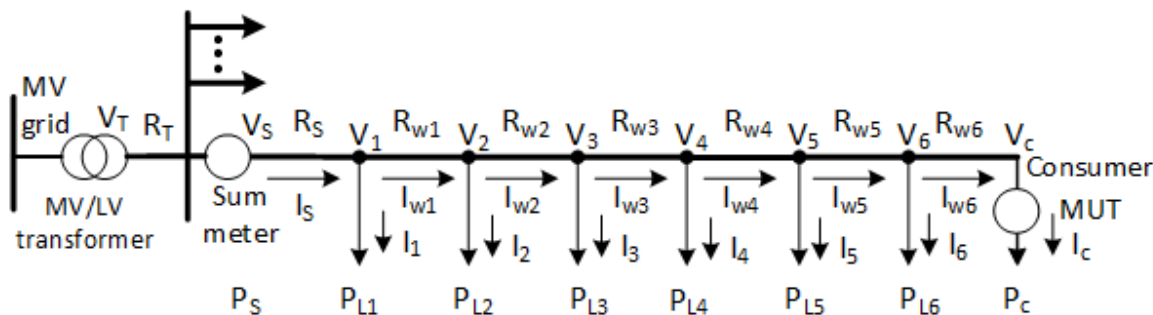


Figure 1. Equivalent circuit representing the energy delivery route from sum meter to consumer MUT. The arrows and dots represent the other branches. The circles represent electricity meters.

The section of the DG between the sum meter installation point and the consumer, which is monitored by the smart meter, includes several branches with active resistances R_{wi} , $i = 1, N$ and loads P_{Li} , $i = 1, N$ as depicted in Figure 1. The electrical quantities at intermediate nodes from 1 to N are not tracked by the consumer MUT. When the power consumption at the consumer node changes by dP_c , the network's power consumption dP_n alters due to change in losses caused by resistances R_{wi} and consumption of loads P_{Li} . We assume that choosing $N = 6$ adequately captures the effect of branch resistances and various other consumer loads to examine the dP_n range accessible to readings at the sum and consumer MUT locations. If the consumer MUT is not connected at the DL's beginning, all DL in front of the consumer MUT can be represented by the N th node's appropriate power consumption.

2.2. Data Synthesis

To validate the proposed model for estimating dP_n , the electrical flow issue was resolved for the circuit depicted in Figure 1, utilizing the pandapower (version 3.1.2) tool (<https://www.pandapower.org/>, accessed on 14 June 2025). In the simulations, the MV/LV transformer was represented by the 0.25 MVA, 10/0.4 kV transformer model from the standard pandapower library. The scenarios of DL resistances (Figure 1) are provided in Table 2. Table 3 presents cases of the active power loads of the network.

Table 2. Resistances of distribution lines.

Grid Case	R_s , mΩ	R_{w1} , mΩ	R_{w2} , mΩ	R_{w3} , mΩ	R_{w4} , mΩ	R_{w5} , mΩ	R_{w6} , mΩ	R_{wsum} , mΩ
1	30	30	30	30	30	30	30	210
2	30	15	15	15	30	30	30	165
3	30	30	30	30	15	15	15	165

Table 3. Active power load cases.

Grid Load Case	P_{L1} , kW	P_{L2} , kW	P_{L3} , kW	P_{L4} , kW	P_{L5} , kW	P_{L6} , kW
1	0	0	0	0	0	0
2	6	0	0	0	0	0
3	6	6	0	0	0	0
4	0	0	0	6	0	0
5	0	0	6	6	0	0
6	0	0	0	0	0	6
7	0	0	0	0	6	6
8	6	6	6	6	6	6

The synthesized data covers variety scenarios in order to assess the main effects of the branch operational modes on the method performance including different branch parameters, different loading patterns and uneven load distribution along the branch, different load types and different sizes of the consumer power step. Combination of the loads and wire resistances during the worst-case scenario, i.e., grid case 1 presented in Table 2, together with grid load case 8 presented in Table 3, causes 10% voltage drop in the power supply path. The other grid load cases were meant to consider the effect of unequal line lengths between consecutive loads. Grid load cases presented in Table 3 were utilized to assess the effect of different voltage drops and power losses in the branch.

The arrangement of network load powers, smart meters metered power, and the consumer power step size of $dP_c = (0.3, 0.5, 0.7, 1.0, 1.5)$ kW, to cover the relevant power ranges of the conventional household appliances, alongside the power consumption preceding the power step of $P_{c1} = (0, 0.3, 0.6, 0.9, 1.2)$ kW, is depicted in Figure 2, accompanied by the corresponding dP_n for each configuration scenario. The network loads were simulated using the ZIP model, encompassing both constant impedance (ZZ) and constant power (ZP) coefficients, with $ZP = 1 - ZZ$ within this model. Every load P_{Li} , $i = 1, N$, assumed the constant impedance coefficient as illustrated in Figure 2. The aggregate power consumption of the DG branch is

$$P_{eqn} = \sum_{i=1}^N P_{Li} + \sum_{i=1}^N P_{wi} + P_{Rs} \quad (5)$$

where P_{wi} and P_{Rs} represent the power losses within the i th energy delivery branch and the R_s branch, respectively. The distribution of P_{Li} , along with its metadata, is available at https://github.com/KTU-ANODETEL/Grid_of_6_Nodes_One_Phase_Dataset1, accessed on 14 June 2025.

This study initially focusses on the consumption of active power by consumer loads. Future plans include adapting the method to account for both active and reactive power components.

As shown in Figure 2, the values of dP_n can exhibit both positive and negative variations dependent upon the nature of loads and the magnitude of technical losses within the DG branches. This inherent complexity renders the prediction of dP_n a challenging task. Furthermore, it is evident that fluctuations in dP_n are substantial, and employing the conventional average power loss rate (commonly approximately 4 to 5% of power consumption in LV grids) in lieu of the actual dP_n would significantly impair the accuracy of power balance equality (Equation (1)). Notably, the ratio of the alteration in PCC in distribution branch to consumer's PCC $k_n = (dP_n/dP_c) \cdot 100\%$ oscillated between -5% and $+15\%$, contingent on the load configuration (refer to Figure 2).

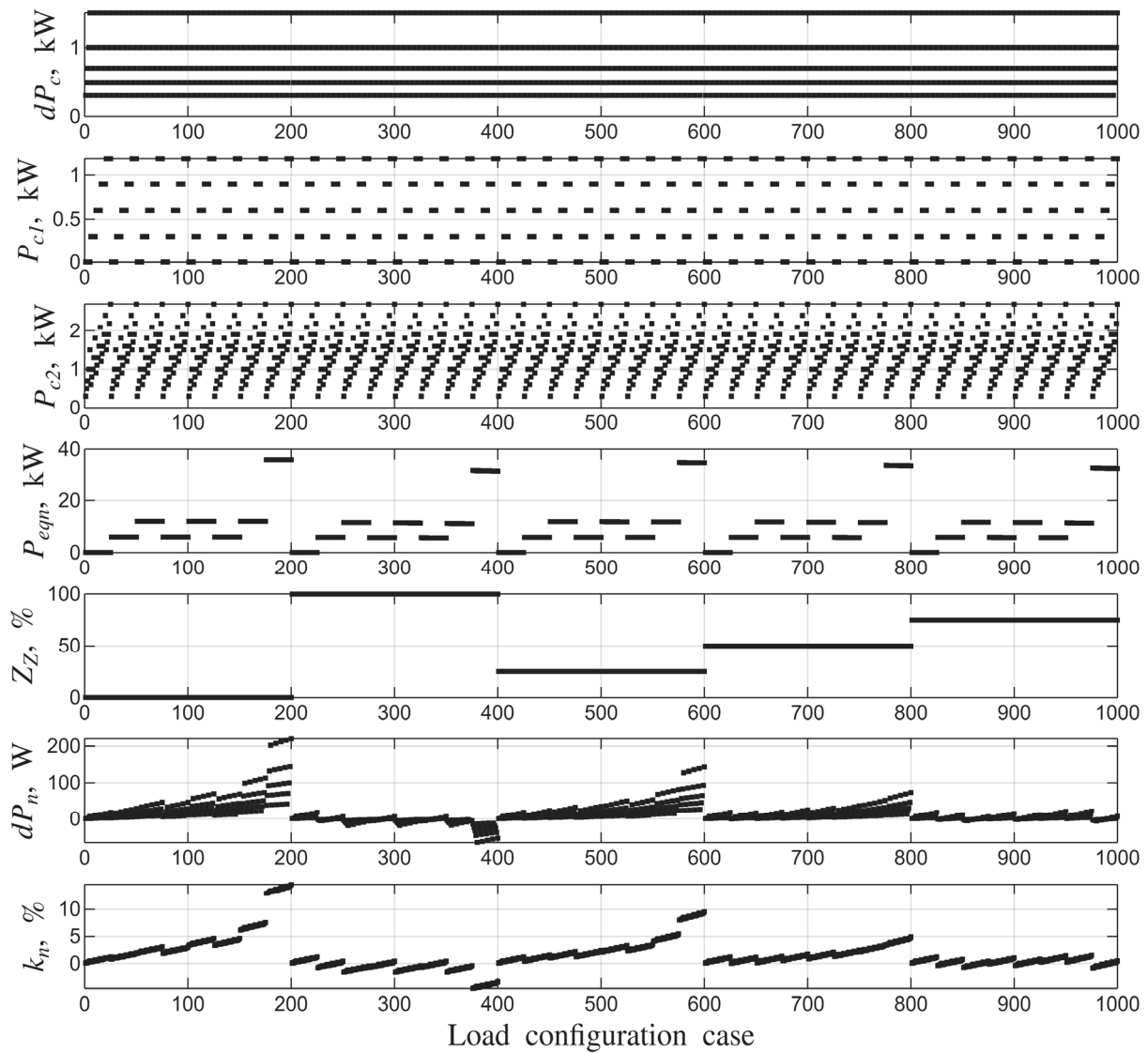


Figure 2. Consumer load power, DG branch power consumption, ZIP model coefficient of loads, change of DG branch power consumption after consumer power event, and power losses coefficient in the synthesized data obtained from grid configuration case no. 2 (Table 2).

2.3. Meter Error and Resolution Modelling

Readings of electrical quantities acquired by consumer and sum meter exhibit measurement errors, including those caused by limited resolution compared to error-free synthesized data. We assume the following model of current and voltage readings

$$I = I_0 \cdot \left(1 + \frac{E_I}{100\%} \right) \quad (6)$$

$$V = V_0 \cdot \left(1 + \frac{E_V}{100\%} \right), \quad (7)$$

where I_0 and V_0 are error-free values of the current and voltage obtained during synthesis, E_I and E_V are the relative percentage gain errors of current and voltage, respectively.

The gain error can be divided into systematic components (e_I , e_V) and random components (r_I , r_V), such that:

$$E_I = r_I + e_I; E_V = r_V + e_V. \quad (8)$$

The systematic relative gain error is more related to the aging of the meter and the influence of environmental conditions. The random component of the gain error represents higher frequency thermal noise caused due to the electrical components in the measurement channel of the current and voltage.

In a similar way, the active power readings can be modelled by

$$P = I \cdot V \cdot \cos\varphi = I_0 \cdot \left(1 + \frac{E_I}{100\%}\right) \cdot V_0 \cdot \left(1 + \frac{E_V}{100\%}\right) \cdot \cos\varphi. \quad (9)$$

We do not consider phase angle measurement errors in this research. It can be derived from (6)–(8) that:

$$P = I_0 \cdot V_0 \cdot (1 + e_P + r_P) \cdot \cos\varphi \quad (10)$$

where systematic gain error and random gain error of active power measurement are correspondingly denoted

$$e_P \approx \frac{e_I}{100\%} + \frac{e_V}{100\%}, \quad (11)$$

$$r_P \approx \frac{r_I}{100\%} + \frac{r_V}{100\%}, \quad (12)$$

when lower order terms such as $e_V \cdot e_I / (100\% \cdot 100\%)$, $e_V \cdot r_V / (100\% \cdot 100\%)$, $r_V \cdot e_I / (100\% \cdot 100\%)$, and $r_V \cdot r_I / (100\% \cdot 100\%)$ are neglected. Later, relative errors expressed in parts rather than percent will be used

$$\gamma_I = \frac{e_I}{100\%}, \quad (13)$$

$$\gamma_V = \frac{e_V}{100\%}, \quad (14)$$

$$\delta_I = \frac{r_I}{100\%}, \quad (15)$$

$$\delta_V = \frac{r_V}{100\%}. \quad (16)$$

The accuracy class of an energy meter (0.2, 0.5, 1, and 2 according to the standards IEC 62053-21 and IEC 62053-22) defines the allowed range of power measurement errors. Class 1 m are subject to a maximum error of $\pm 1\%$ of the measured active power value. The presented research focusses on identifying changes in gain error, while the random component of gain error is presumed to be constant. For example, if current and voltage systematic gain errors are equal to 0.5% and random gain errors equal to 0.5% (rectangular distribution), then the power systematic gain error will be 1% and the power gain error will not exceed the range between 0 and 2%.

In a real-life application, the average of K measurement samples will be used to estimate the power, current, and voltage of the sum and consumer MUT before and after the power event (Figure 3). Therefore, the variance of random component will be reduced \sqrt{K} times due to the averaging operation. In the research that follows, K is set to 10.

While active power calculations in meter metrology modules are performed with high resolution, quantity readings are presented on the meter display or transmitted through communication channels with a restricted resolution. To represent the constrained resolution of quantity readings, such as current, an expression is utilized

$$I_{read} = \text{round}\left(\frac{I}{res}\right) \cdot res \quad (17)$$

where res denotes the current resolution in current units, I represent the high-resolution current, and I_{read} stands for the current reading displayed with the resolution res . For

instance, if I is 1.457 A and res is 0.01 A, then I_{read} would be 1.46 A. The resolution error is inherently random, with a zero mean and a uniform distribution.

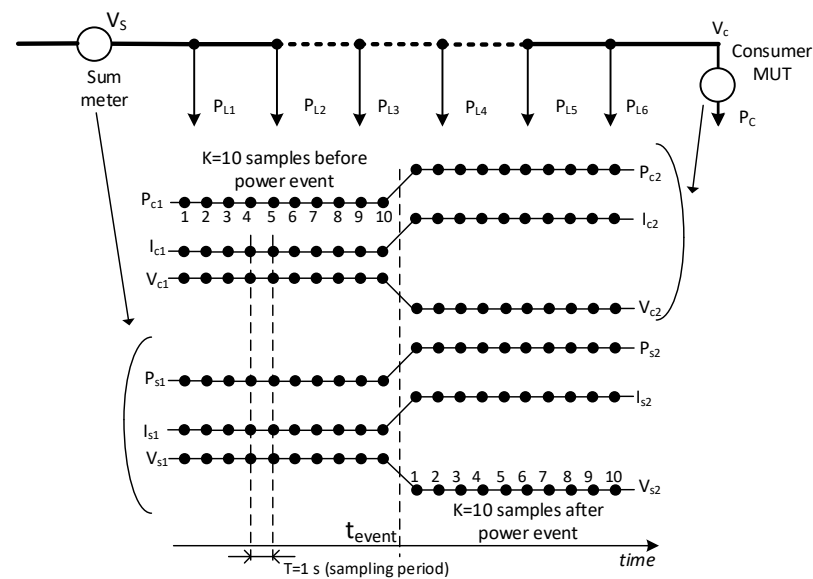


Figure 3. Power, current, and voltage readings of sum meter and consumer MUT before and after power event.

Random and systematic type errors influence the readings of both meters (sum and consumer). Errors occur in both voltage, current, and power readings. In this study, we will assume that the random type errors of power measurement are equal to the accuracy classes of typical meters. At the same time, we will also evaluate the influence of resolution. Limited resolution affects both current, voltage, and power readings. The numerical values of the resolution are taken according to the capabilities of the P1 interface (the P1 port is a device of smart electricity meters) of currently used typical meters. The values of the random errors and resolutions studied are presented in Table 4. The influence of systematic type errors will be investigated in the range from -5% to $+5\%$ (when evaluating consumer power data readings).

Table 4. Meter class and random error (r_p) of active power measurement.

Case	Sum Meter Class	Sum Meter, Random Power Error (r_p), %	Consumer Meter, Class	Consumer Meter, Random Power Error (r_p), %	Sum Meter Voltage, Current and Power Readings Resolution	Consumer Meter Voltage, Current and Power Readings Resolution
M1	0	0	0	0	0.1 V, 0.05 A, 1 W	0.1 V, 0.05 A, 1 W
M2	0.5	0.5	0.5	0.5	0.1 V, 0.05 A, 1 W	0.1 V, 0.05 A, 1 W
M3	0.5	0.5	1	1	0.1 V, 0.05 A, 1 W	0.1 V, 0.05 A, 1 W

2.4. Synthesized Training and Testing Datasets

The synthesized data are partitioned into training and testing datasets. Using Equations (6)–(12): (1) random noise corresponding to meter class is added to the sum and consumer current, voltage and active power readings of training and testing datasets before and after the consumer power event (Figure 3), (2) systematic gain error is injected into the testing set of only consumer meter readings in the (6)–(12), (3) finally, the resolution is restricted in all datasets by applying (17).

The notations of the synthesized data with the injected random and systematic gain errors is denoted in Figure 3. The index 1 denotes average (from K samples) power, current

and voltage before the power event, and index 2 denotes average (from K samples) power, current and voltage after the power event.

In Table 5, cases of training and testing datasets are assigned distinctive titles (T1, T2, T3) for the faster reference in the following text. Odd samples from the complete synthesized dataset (Figure 2) of power, current and voltage are always used to build data-driven models (training phase), which will be used to predict PCC and estimate gain error of consumer MUT. The test data set was composed from even samples of the full dataset or by selecting other samples according to the rule listed in Table 5.

Table 5. Cases of training and testing synthesized datasets (total number of samples and percentage of the full dataset).

Dataset Case	Training Data Set	Testing Data Set
T1	500 samples/50% (odd samples, sample numbers $2n - 1$, n is integer number from 1 to $N/2$)	500 samples/50% (even samples, sample numbers $2n$, n is integer number from 1 to $N/2$)
T2	500 samples/50% (odd samples)	250 samples/25% (sample numbers $4n$, n integer number from 1 to $N/4$)
T3	500 samples/50% (odd samples)	125 samples/12.5% (sample numbers $8n$, n integer number from 1 to $N/8$)

To summarize, the dataset was generated:

- (1) Setting power consumption such that to cover ranges of typical loads used at households of residential consumers
- (2) Modeling equivalent network to obtain voltage and current corresponding to the power consumption before the power step and after power step at the consumer site which is metered by consumer MUT. Different distribution branch resistances were used to generate data sets representing distribution networks with different wiring resistances (losses)
- (3) Injecting random and systematic errors into simulated I/V/P according to (6), (7) and (10)
- (4) Limiting resolution of V/I/P readings to represent limited resolutions of readings available from smart meters over communication interfaces.

Despite the wiring resistances and power consumptions might be slightly different depending on countries, historical period of electrical network construction, contracts between consumers and utilities in different countries, but absolute values are not particularly critical for the verification of the performance of a suggested method for PCC in the branch and meter gain error detection. This is a typical research methodology in electrical power systems when some standard, equivalent, typical network and their parameters are used to verify a developed measurement, detection, control, or similar methods.

3. A Technique for Prediction of Branch Power Consumption Change

To determine the PCC of distribution grid dP_n a two steps approach is applied. First, in the reference conditions when sum and smart meter readings are trusted to be within their accuracy class limits, the so-called training phase is performed. Assuming the equivalent DG branch schematic as shown in Figure 4, the equivalent resistance R_{eq} is estimated and a data-driven model for dP_{nL} prediction using consumer meter readings is derived (see also (2)). P_{eqn} aims to model the total of all loads connected in the DG branch (P_{Li} , $i = \overline{1,6}$ in Figure 1). dP_{nL} denotes PCC of P_{eqn} after a consumer power event.

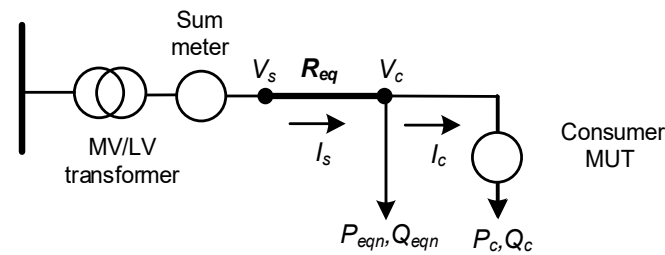


Figure 4. Equivalent circuit of the branch of distribution grid.

Second, in a testing (or monitoring) phase, dP_n is estimated using average R_{eq} and dP_{nL} prediction model. These two procedures are described in detail below.

In the training phase using training dataset, estimates of R_{eq} and dP_{nL} are determined:

1. The equivalent resistance R_{eq} is calculated according to expression

$$R_{eq} = \frac{dV_c - dV_s}{dI_s}, \quad (18)$$

where $dV_s = V_{s2} - V_{s1}$ represents voltage change, and $dI_s = I_{s2} - I_{s1}$ denotes the current change measured by the sum meter. Similarly, $dV_c = V_{c2} - V_{c1}$ corresponds to the voltage change measured by the consumer's meter.

After processing a set of consumer load changes, the mean value $\overline{R_{eq}}$ is calculated.

2. A data-driven linear regression model for predicting dP_{nL}

$$d\hat{P}_{nL} = f(V_{c2}, V_{c1}, P_{c2}, P_{c1}) \quad (19)$$

is built using stepwise regression (Matlab `stepwiselm` training function) with the target attribute obtained from training data using equation

$$dP_{nL} = dP_s - dP_c - dP_w = (P_{s2} - P_{s1}) - (P_{c2} - P_{c1}) - \frac{(V_{s2} - V_{c2})^2 - (V_{s1} - V_{c1})^2}{\overline{R_{eq}}}, \quad (20)$$

and predictor variables including voltage and active power after and before the power event V_{c2} , V_{c1} , P_{c2} , P_{c1} and their following multiplications $V_{c2} \cdot V_{c1}$, $V_{c2} \cdot P_{c2}$, $V_{c2} \cdot P_{c1}$, $V_{c1} \cdot P_{c2}$, and $V_{c1} \cdot P_{c1}$ that were selected by the training function as the most relevant predictors. The set of predictors (input features) was determined using the dataset synthesized T1 (see Table 5) and M3 (see Table 4) cases and afterwards was maintained fixed for other examined training datasets. The model (19) exhibited a coefficient of determination (R-squared) equal to 0.989. This way we attempt to avoid variations of model's structure dependent on training data, because we do not have any evidence or expectation that underlying phenomena are influencing relationships between physical quantities somehow differ when synthesizing different data sets using the same equivalent circuit. No other non-default settings were chosen for the regression model training.

In the testing (or monitoring) phase, smart meter current, voltage, and power gain errors can appear, and they influence dP_n estimation error. Therefore, dP_n estimation and consumer meter gain error estimation cannot be solved separately. Using the balance equation gain error and afterward dP_n can be evaluated. Since both quantities are solved in the testing phase, the higher quality of dP_n prediction positively influence precision of gain error estimation. Therefore, dP_n estimation error minimization and lower sensitivity to both meters random and systematic errors remains relevant, though itself it is not the final goal of monitoring.

1. Assuming that the relative systematic error of consumer meter is γ_V , the predicted power losses within the DG branch can be expressed as:

$$d\hat{P}_w = \left(V_{s2} - V_{c2}/(1 + \gamma_V) \right)^2 - \left(V_{s1} - V_{c1}/(1 + \gamma_V) \right)^2 / \overline{R_{eq}}. \quad (21)$$

The predicted PCC of network loads is evaluated using the model (19) derived in training phase and using corrected predictor readings:

$$d\hat{P}_{nL} = f \left(\frac{V_{c2}}{1 + \gamma_V}, \frac{V_{c1}}{1 + \gamma_V}, \frac{P_{c2}}{1 + \gamma_I + \gamma_V}, \frac{P_{c1}}{1 + \gamma_I + \gamma_V} \right). \quad (22)$$

The predicted quantity of the change of the sum meter PCC in response to a consumer load change can be expressed:

$$d\hat{P}_s = d\hat{P}_w + d\hat{P}_{nL} + \frac{P_{c2}}{(1 + \gamma_I + \gamma_V)} - \frac{P_{c1}}{(1 + \gamma_I + \gamma_V)}. \quad (23)$$

To estimate the systematic gain errors of voltage and current $S_{IV} = (\hat{\gamma}_I, \hat{\gamma}_V)$ or their expression in percentage $S_{IV} = (\hat{e}_I, \hat{e}_V)$ it is necessary to solve the following minimization problem:

$$S_{IV} = \min \left(\sum_{i=1}^M (d\hat{P}_s(i) - dP_s(i))^2 \right), \quad (24)$$

where index i denotes the number of power event, and M is the total number of power events, $dP_s = P_{s2} - P_{s1}$ is the sum meter measured PCC.

The solution of problem (24) is achievable using the least squares minimization solver.

The absolute estimation error of the systematic gain error of voltage (current or active power) is defined as

$$\Delta(e_V) = \hat{e}_V - e_V, \quad (25)$$

where e_V represents the actual gain error associated with voltage (the same for current, or active power measurements), as established during the synthesis of the test data set. Standard deviation $\sigma(\Delta(e_V))$ of mean is a typical measure of repeatability of the estimation error.

2. The predicted $d\hat{P}_n$ can be found by substituting systematic error of voltage and current with their estimates correspondingly $\hat{\gamma}_V$ and $\hat{\gamma}_I$ in (21), (22) and the expression

$$d\hat{P}_n = d\hat{P}_w + d\hat{P}_{nL}. \quad (26)$$

The mean value $\overline{d\hat{P}_n}$ is obtained by averaging predictions $d\hat{P}_{ni}$, $i = \overline{1, M}$ that were obtained using voltage, current and power readings corresponding to i th power event.

4. Performance Assessment of Branch Power Change Estimation

4.1. Distribution Branch Resistance Estimation

Figure 5 presents the estimations of R_{eq} derived from the testing dataset, along with the relative error

$$e(R_{eq}) = \frac{R_{wsum} - R_{eq}}{R_{wsum}} \cdot 100\%, \quad (27)$$

where $R_{wsum} = \sum_{i=1}^N R_{wi} + R_S$ represents the sum of DL resistances in the energy delivery pathway.

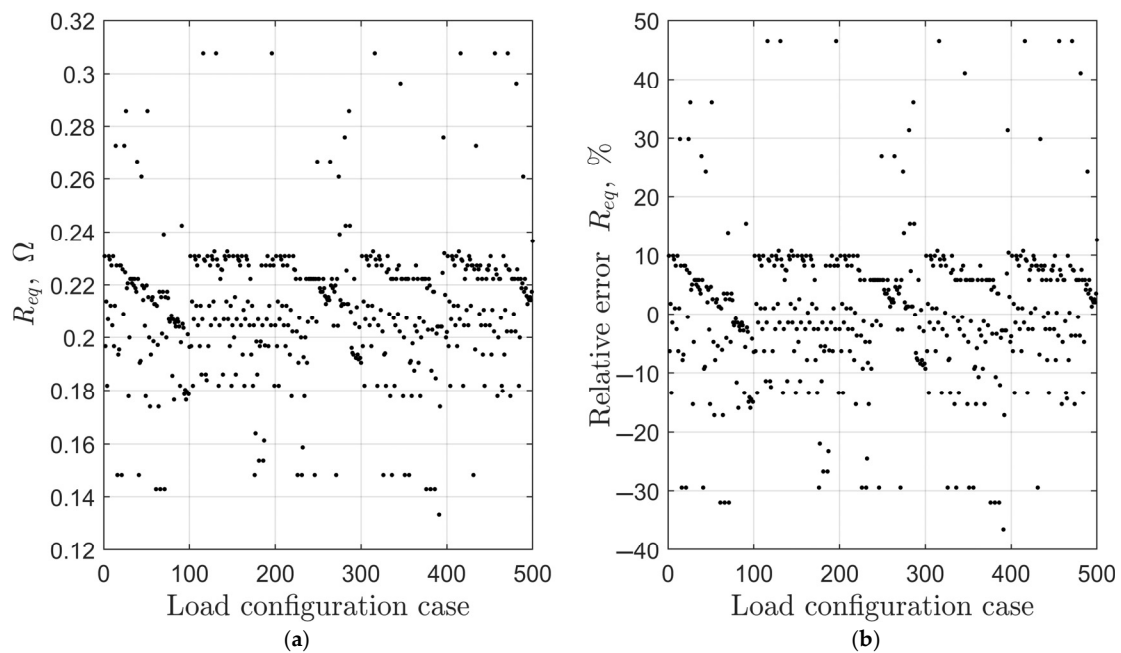


Figure 5. R_{eq} (a) and relative error of its estimate (b) vs. grid loads configuration case (see Table 3 and Figure 2). Grid case no. 1 from Table 2.

The mean value of $\overline{R_{eq}}$ was determined based on distinct network configurations. Its relative error $e(\overline{R_{eq}})$ and the standard deviation $\sigma(e(\overline{R_{eq}}))$ of estimation error mean are presented in Table 6. Despite that an estimate of R_{eq} exhibits rather high estimation error, but the average of M estimate yields a good match to the actual branch resistance R_{wsum} .

Table 6. Equivalent resistance estimation. Meter class and random power error case M1 from Table 4 and training data T1 from Table 5.

Grid Case	R_{wsum} , m Ω	$e(\overline{R_{eq}})$, %	$\sigma(e(\overline{R_{eq}}))$, %
1	210	0.64	0.56
2	165	1.66	0.76
3	165	1.37	0.73

4.2. Network Power Consumption Change After the Consumer Power Event

The prediction of change in power losses of DG branch denoted as $d\hat{P}_w$ is estimated using (26) (see Figure 6), whereas the actual dP_w can be obtained from testing data readings according to definition (see quantities notation in Figure 1)

$$dP_w = \sum_{i=1}^N dP_{wi} + dP_{Rs} = \sum_{i=1}^N dI_{wi}^2 R_{wi} + dI_s^2 R_s. \quad (28)$$

The prediction of change in grid loads power consumption $d\hat{P}_{nL}$ is estimated using (22) (see Figure 7), whereas the actual dP_{nL} can be obtained from testing data readings according to definition (see quantities notation in Figure 1)

$$dP_{nL} = \sum_{i=1}^N (P_{L(2)i} - P_{L(1)i}) = \sum_{i=1}^N dP_{Li} \quad (29)$$

where $P_{L(1)i}$ and $P_{L(2)i}$ are power consumption of the i th consumer before and after the power event respectively.

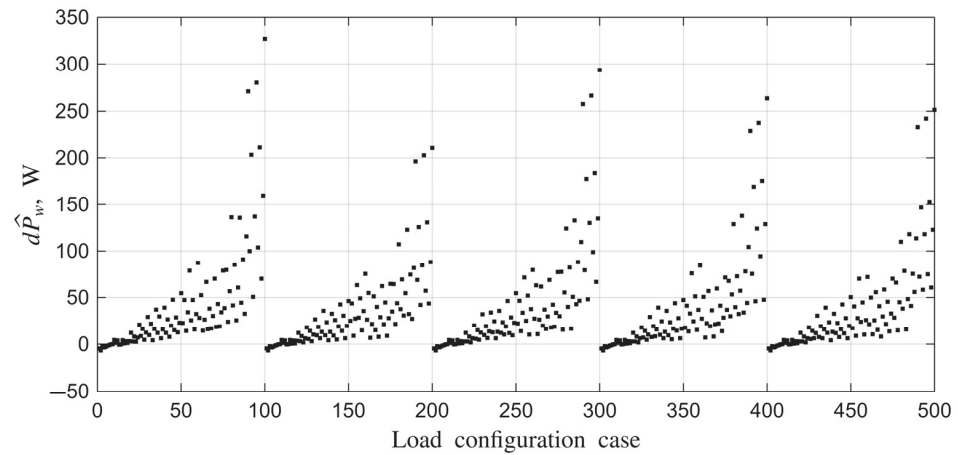


Figure 6. Predicted DG branch power loss change $d\hat{P}_w$. Grid case no. 1 from Table 2. Meter class and random power error case M1 from Table 4 and training/testing data set case T1 (Table 5).

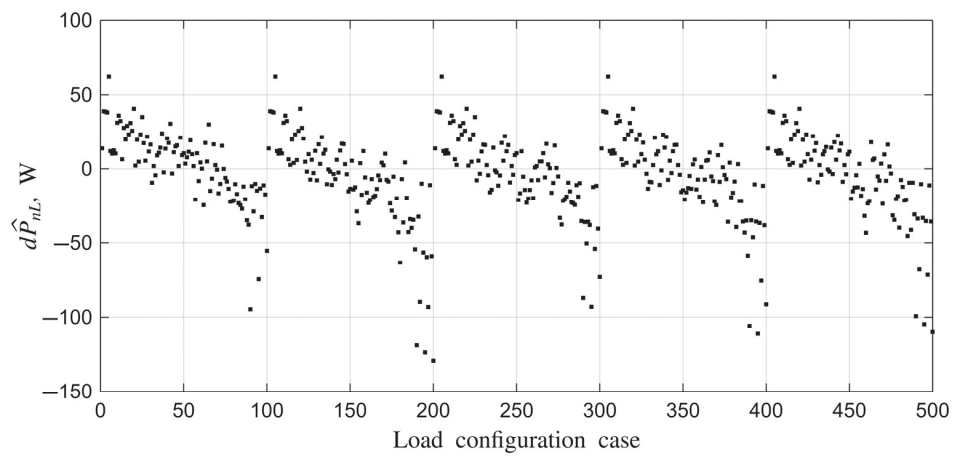


Figure 7. Predicted network loads change $d\hat{P}_{nL}$. Grid case no. 1 from Table 2. Meter class and random power error case M1 from Table 4 and testing data (50% (even) of data).

The overall predicted PCC in the DG branch $d\hat{P}_n$ is estimated using (26), whereas it's the actual dP_{nL} is calculated from testing data set

$$dP_n = dP_w + dP_{nL} \quad (30)$$

The absolute error of prediction of $d\hat{P}_n$ is

$$\Delta(d\hat{P}_n) = dP_n - d\hat{P}_n \quad (31)$$

The predicted PCC $d\hat{P}_n$ and its prediction error $\Delta(d\hat{P}_n)$ are shown in Figure 8.

The average $\overline{d\hat{P}_n}$ calculated from all estimated samples of $d\hat{P}_n$ which are obtained using testing dataset are shown in Table 7 along with relative error average,

$$e(\overline{d\hat{P}_n}) = \frac{\overline{d\hat{P}_n} - \overline{dP_n}}{\overline{dP_n}} \cdot 100\%, \quad (32)$$

the standard deviation $\sigma(\Delta(d\hat{P}_n))$ of absolute error $\Delta(d\hat{P}_n)$ values, and the relative errors of $\overline{dP_n}$

$$e(\sigma(\Delta(d\hat{P}_n))) = \frac{\sigma(\Delta(d\hat{P}_n))}{\overline{dP_n}} \cdot 100\%, \quad (33)$$

where $\overline{dP_n}$ denotes average of actual dP_n values in the testing dataset.

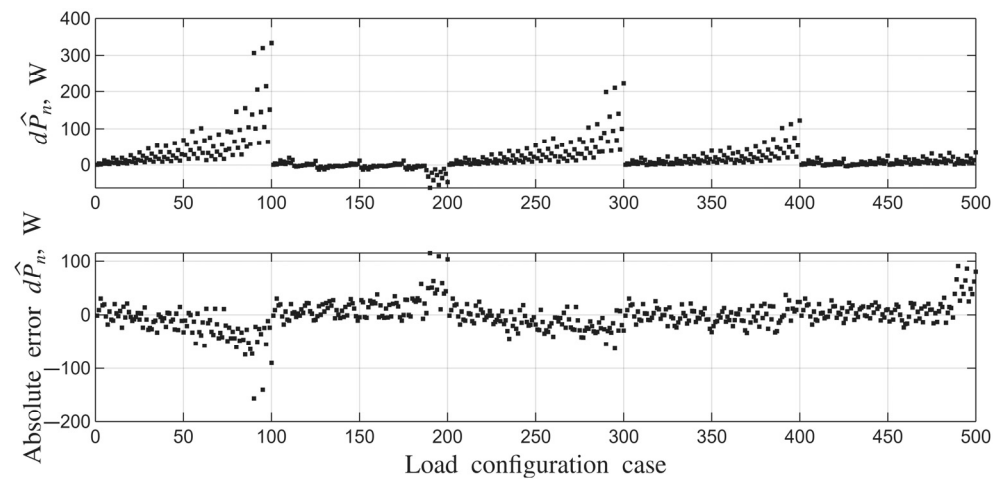


Figure 8. Predicted PCC in the branch $d\hat{P}_n$ and its prediction error. Grid case no. 1 from Table 2. Meter class and random power error case M1 from Table 4 and testing data (50% of samples (even)).

Table 7. $\overline{d\hat{P}_n}$ estimation performance. $e_I = 0\%$, $e_V = 0\%$, $e_P = 0\%$. Data: grid case no. 1 from Table 2.

Training/Testing Data Case	Meter Class and Random Power Error (r_P) (Table 4)	$\overline{d\hat{P}_n}$, W	Standard Deviation of $\overline{d\hat{P}_n}$, W	Relative Error of $\overline{d\hat{P}_n}$, %	Standard Deviation of Relative Error $\overline{d\hat{P}_n}$, %
T1	M1	21.5	— ²	−5.51	— ²
T1	M2 ¹	21.7	1.8	−4.37	7.8
T1	M3 ¹	22.0	2.2	−3.20	8.9
T2	M1	21.3	— ²	−3.94	— ²
T2	M2 ¹	20.2	3.6	−8.80	16.0
T2	M3 ¹	21.6	1.9	−2.71	8.8
T3	M1	21.3	— ²	0.21	— ²
T3	M2 ¹	20.1	2.3	−5.37	10.9
T3	M3 ¹	21.0	2.3	−1.45	10.9

¹ 10 iterations were performed using M2 and M3 cases with different noise ensembles. ² In these cases standard deviation of $\overline{d\hat{P}_n}$ and standard deviation of relative error $\overline{d\hat{P}_n}$ are not calculated.

The results in Table 7 were obtained in the case where systematic errors were absent in the readings of the consumer MUT. It can be seen that the ratio between training data set size and testing data set size does not significantly influence the standard deviation of prediction error of $\overline{d\hat{P}_n}$. Also, no strong correlation was observed between random error influenced by meter accuracy class of power measurement and error of prediction of $\overline{d\hat{P}_n}$.

By analyzing relative error of $\overline{d\hat{P}_n}$ and its standard deviation in Table 7, it cannot be confirmed that higher accuracy class of consumer meter (compare M2 and M3 cases) yields higher accuracy of PCC prediction. Moreover, we have observed that less random noise level due to better meter accuracy class may cause higher PCC estimation error (compare case T2/M2 to T2/M3). This could be explained that training data containing higher levels (to some extent, of course) of additive random noise is better generalized by the data-driven model (19) and consequently more accurate prediction of $d\hat{P}_s$ according to (23). Though more extensive analysis might be required, but our initial insight is that improvement of consumer meter accuracy class does not unequivocally improves PCC in the branch prediction error due to the influence of other factors impacting solution of minimization problem (24) which is necessary to obtain estimates of voltage and current gain errors and afterwards PCC using (21), (22) and (26).

4.3. Influence of Systematic Gain Errors of Consumer MUT

Figure 9 presents scatter plots of e_I , e_V , e_P estimations, which are obtained by solving (24). It indicates a good approximation precision.

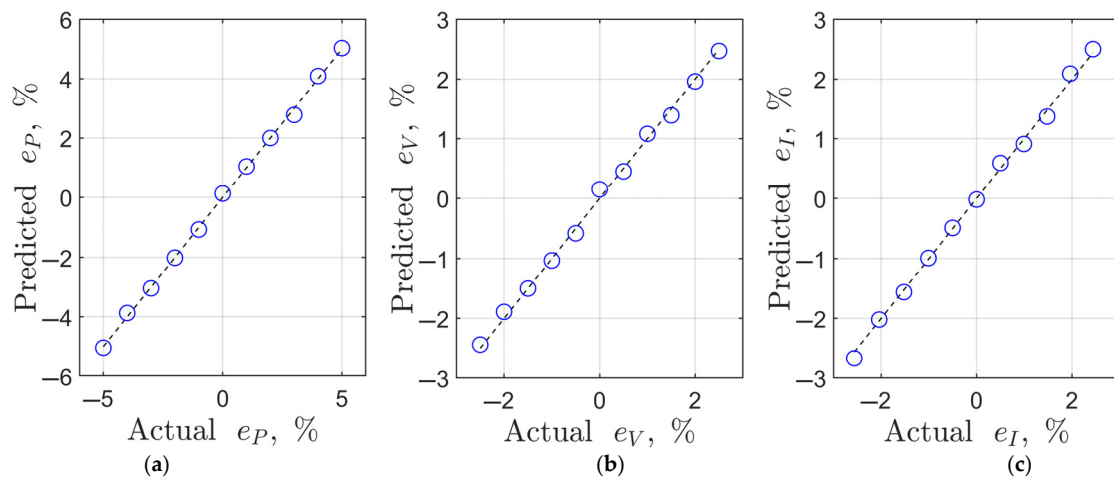


Figure 9. Scatter plots of gain errors e_P (a), e_V (b), e_I (c) estimates. Test data: grid case no. 1 from Table 2, Meter class and random power error case M3 and Training data/Testing data case T3 from Table 7.

It can be seen from Figure 10a that the $\overline{d\hat{P}_n}$ estimation error is not influenced by the size of e_P increases in case of larger estimation error of e_P (see Figure 10b).

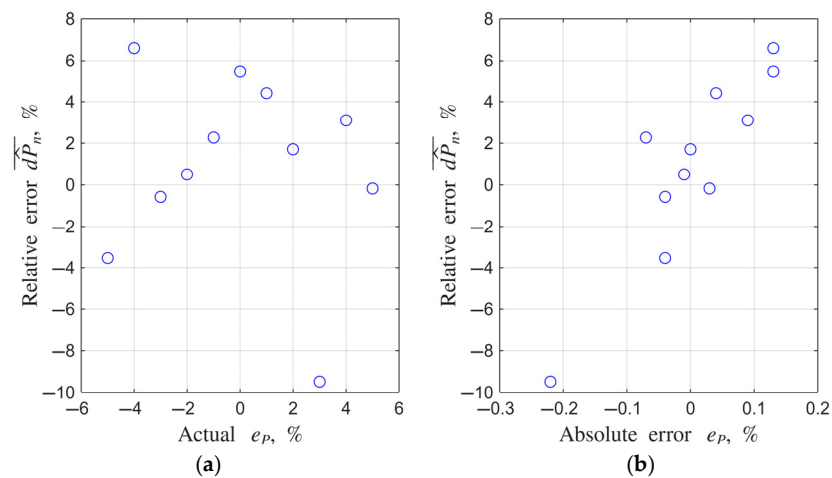


Figure 10. Relative error of $\overline{d\hat{P}_n}$ versus e_P actual value (a) and versus absolute e_P estimation error of $\Delta(\hat{e}_P)$ (b). Every sample of relative error of $\overline{d\hat{P}_n}$ was obtained by averaging 10 estimates $d\hat{P}_n$ acquired at 10 different noise ensembles of random injected error. The training/testing data set is T1 from Table 7.

Based on the applied test data set, the RMSE of \hat{e}_P was 0.10%, the RMSE of \hat{e}_V was 0.08%, and RMSE of \hat{e}_I was 0.07% (calculated from estimates shown in Figure 9). From the data shown in Figure 9 it was observed that the absolute error of the estimate of power measurement gain error was within $\pm 0.3\%$. These performance metrics seem quite acceptable for practical needs because Class 1 m power (energy) measurement error should not exceed 1% and if consumer MUT power measurement error estimates are obtained with RMSE 0.10%. The rule for triggering detection of MUT non-compliance to standard requirements could be a fixed threshold-based or adaptive thresholding based on power gain error RMSE calculated after several consecutive estimations.

RMSE of estimation of the relative error of $\overline{dP_n}$ was 4.41% while observed relative error of PCC in the branch samples were within the $\pm 10\%$ range (calculated from estimates shown in Figure 10b, which is superior compared to techniques that neglect the presence of PCC in the branch (neglect the presence means that relative error is 100%).

In Figure 11, the influence of the resistance of the DG branch (grid cases in Table 2) on the absolute error of the estimation of gain error is investigated. Training was performed using the data set corresponding to grid case no. 1, whereas testing data set is indicated in the legend of plots. The training/testing procedure was repeated 10 times, each with different noise samples presenting random error. Ranges $[\bar{e}_{P,V,I} - \sigma(\bar{e}_{P,V,I}), \bar{e}_{P,V,I} + \sigma(\bar{e}_{P,V,I})]$ are indicated in Figure 11 after calculating standard deviation of average $\bar{e}_{P,V,I}$ from $M = 10$ estimates of e_P , e_V , and e_I .

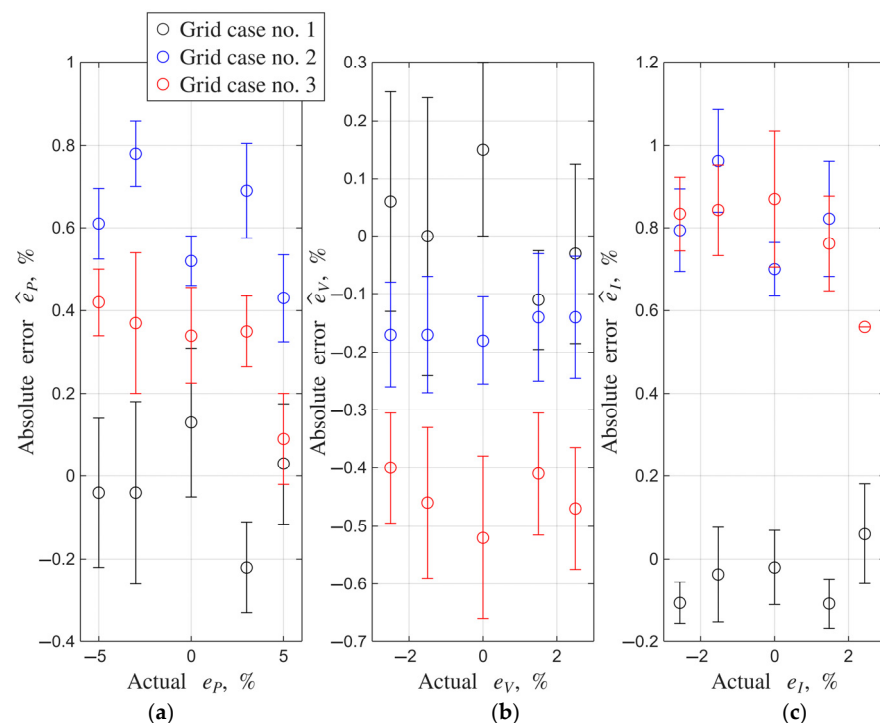


Figure 11. Mean and standard deviation of the mean of absolute error of gain error estimation (e_P (a), e_V (b), e_I (c)). Training was performed using data set corresponding to the T1 dataset of grid case no. 1 and T1 testing data set of the grid shown in the legend of the plot.

It can be seen from results presented in Figures 11 and 12 that change of network losses compared to those present during models' training cause higher estimation errors of both gain error e_P and relative error of $\overline{dP_n}$ estimation. Therefore, it should be acknowledged that the technique suggested for the DG branch PCC in response to consumer load power event is sensitive to the variations in distribution line power losses and the retraining of model (28) might be mandatory to retain better dP_n and low gain error estimation error.

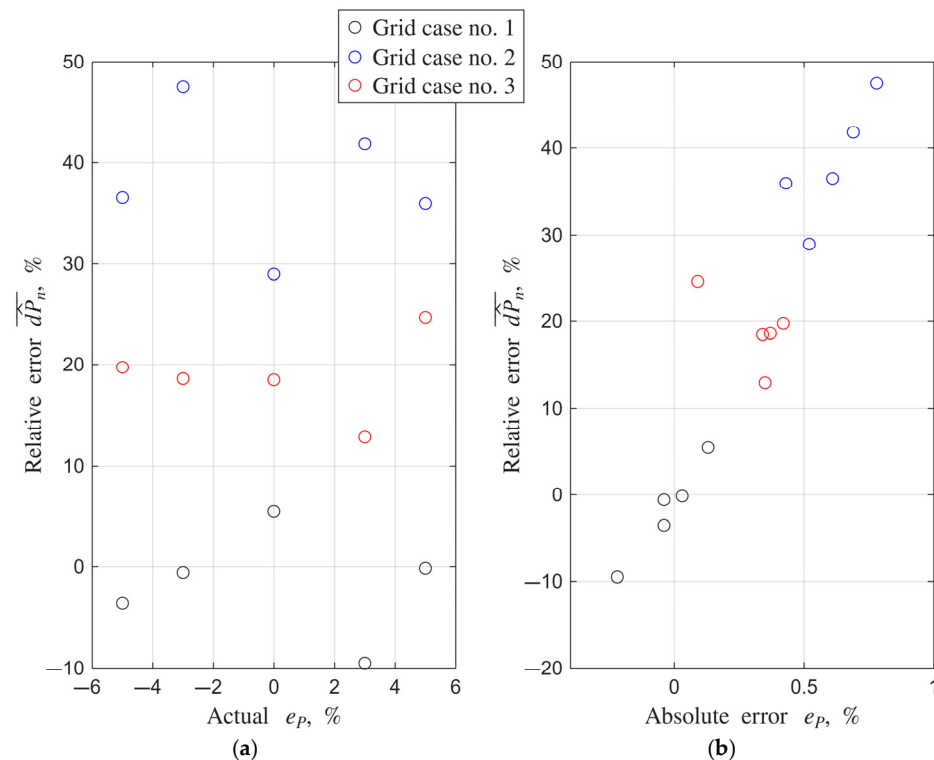


Figure 12. Relative error of $\overline{dP_n}$ estimation versus e_p (a), and versus absolute error of e_p estimation (b). Meter accuracy case M3 and the T3 training data/testing data case from Table 7 are used. Every sample of relative error of $\overline{dP_n}$ was obtained by averaging 10 estimates of dP_n acquired at 10 different noise ensembles of random injected error.

4.4. Experimental Verification

To verify the suggested method a test bed consisting of a sum meter, consumer meter MUT, branch cable R_{eq} , ohmmeter OM, relay control block RB and personal computer for loads control and data collection was constructed (Figures 13 and 14).

The sum meter and the consumer MUT type was Elgama Gama150 Type G15 (<https://www.elgama.eu/G15-en>, accessed on 5 June 2025). Both meters are capable of measuring active power, voltage and current in 1-phase 2-wire networks. Accuracy class B (IEC 50470-3) for active power. Electrical quantities measured by smart meters are transmitted with the period of 1 s via P1 port according to Companion Standard DSMR (Dutch Smart Meter Requirements) ver. 5.0.2, 2016 (<https://www.netbeheernederland.nl/publicatie/dsmr-502-p1-companion-standard>, accessed on 5 June 2025). The resolution of readings in P1 port packets were 0.1 V for a single-phase voltage, 0.001 kW for active instantaneous import power and 1 A for a single-phase current. However, assuming the nominal voltage $V_n = 230$ V and using active power and voltage to calculate current, the achievable current resolution is $0.001 \text{ kW} / 230 \text{ V} \approx 0.005 \text{ A}$. The distribution grid branch resistance R_{eq} was 15 m length with cross-sectional area of 1 mm^2 of copper wire. The actual value of R_{eq} resistance was measured using D.C. Milli-Ohm Meter GOM-802 (OM) with 0.05% accuracy using four-wire measurement mode. To measure R_{eq} using ohmmeter, the R_{eq} was multiplexed using two contact relays K_1 and K_2 . Relays K_3 , K_4 , and K_5 were used to multiplex loads according to a pre-programmed sequence during the experiment. Smart meters and ohmmeter readings were recorded with Matlab R2024b software in personal computer interfaced via P1 (RS-232) to USB converter. To record smart meters messages, interrupt routine was written in Matlab, which was executed on every message received via USB (RS232) for every meter separately. Resistance readings were requested from Ohmmeter (OM). Relays were controlled by relay block (RB) containing the preprogrammed

Arduino Pro Micro microcontroller. All these devices (Smart meters, Ohmmeter and relays) controlled and data recorded using the main Matlab script.

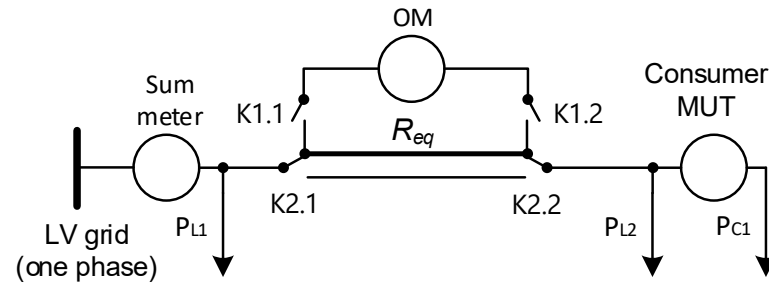


Figure 13. Test bed structural diagram.

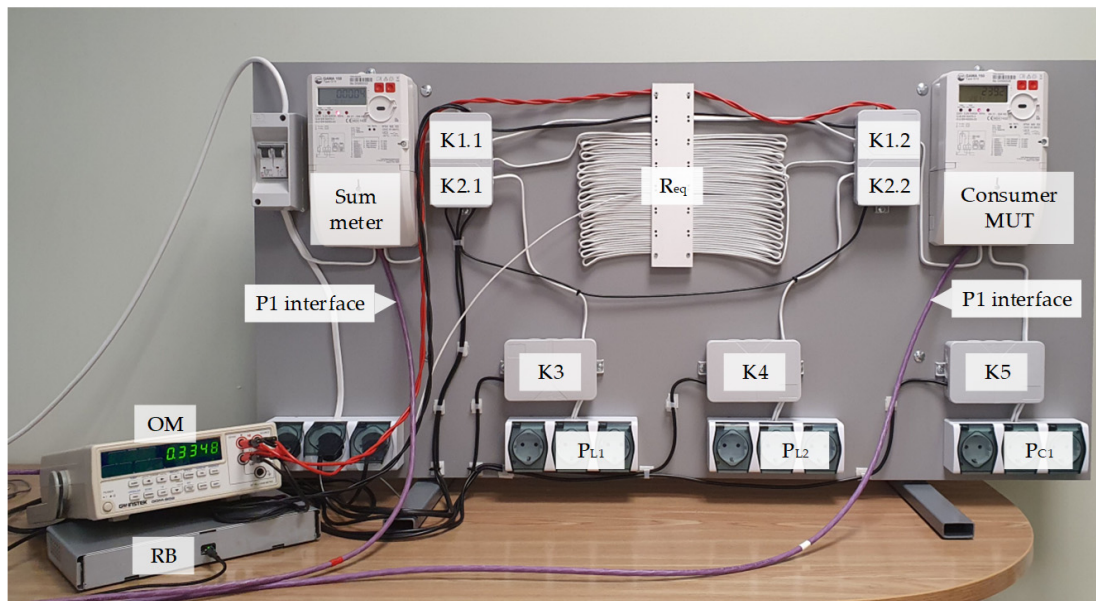


Figure 14. Picture of the test bed for method experimental verification.

The load P_C is switched on and off 10 times with the period of 30 s to generate power event. The total duration of power event recording was approximately 3 h. All loads were of resistive type, their nominal powers were $P_{L1} = (0, 2.0)$ kW, $P_{L2} = (0, 0.4)$ kW, $P_{C1} = (0, 0.25, 0.5)$ kW, and consumer power step sizes were $dP_C = (0.25, 0.5, 0.7, 1.0, 1.5)$ kW. In total 195 power events were recorded with the combinations of initial power consumption of test bed loads shown in Figure 15. According to the circuit shown in Figure 13, a 2 kW nominal power heater is used for implementation of load P_{L1} , a 0.4 kW heater for load P_{L2} , two 0.25 kW incandescent lamp blocks (a and b), a 0.2 kW incandescent lamp (c), and a 0.8 kW heater (d) are used for load P_{C1} . In total, 6 different loads are used. From the loads assigned to P_{C1} , by combining several devices, the power changes dP_C and the constant load P_{C1} are connected every 30 s. For example: the first groups of 5 points shown in Figure 16 correspond to dP_C generated by the following load combinations: group #1—a, group #2—a + b, group #3—a + b + c, group #4—c + d, group #5—a + b + c + d. When loads a and b are used as constant loads (P_{C1} in Figure 15) the last three groups of 5 points shown in Figure 16 correspond to dP_C generated by the following load combinations group #37—c, group #38—d, group #39—c + d.

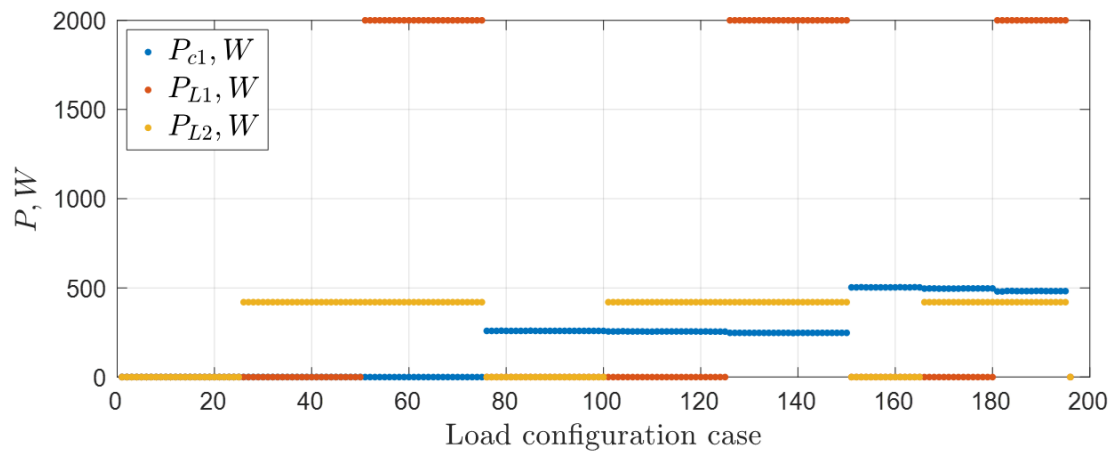


Figure 15. Power consumptions P_{C1} , P_{L1} and P_{L2} .

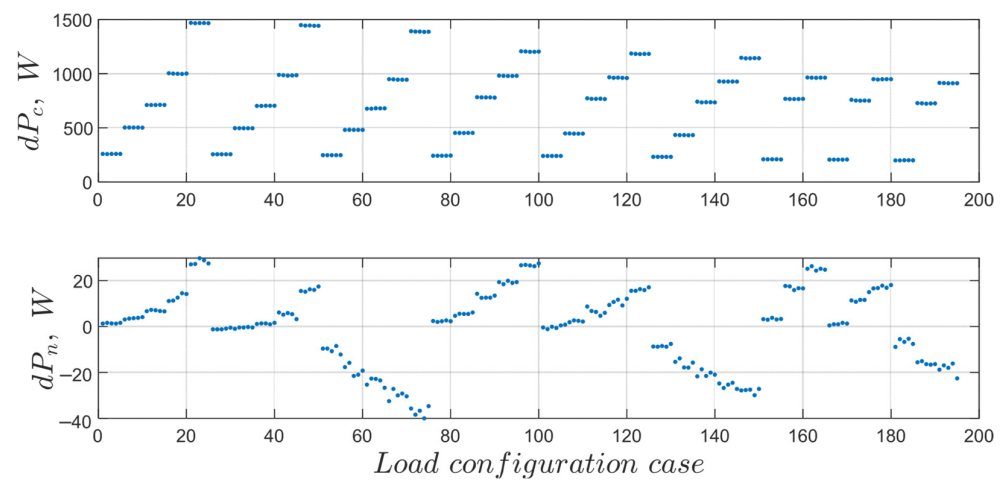


Figure 16. Measured dP_C and calculated dP_n .

For the detection of power step and step size estimation the method presented in [37] was used.

Every power event with the positive magnitude dP_C was repeated 5 times (Figure 16). The value of dP_C is measured by consumer MUT, the value of dP_S is measured by sum meter, and PCC in the branch is calculated as $dP_n = dP_S - dP_C$ (Figure 16).

The resistance R_{eq} is estimated according (18) and samples obtained are plotted in Figure 17. The mean resistance measured using the ohmmeter was 669.08 m Ω , and mean calculated resistance R_{eq} was 667.95 m Ω . Therefore, the mean absolute error $e(\overline{R_{eq}})$ was 0.17% and the standard deviation $\sigma(e(\overline{R_{eq}}))$ of estimation error mean was 3.08%.

All measured samples (195 samples) were split into training and testing data sets. The training data set is always kept the same, and the testing data set cases are shown in Table 8.

In Figure 18, the partitioning of PCC samples for training and testing are displayed.

The training dataset is used to train a model of PCC prediction as described in chapter 3, Equations (18) and (19). In Figure 19, the measured PCC dP_n and predicted PCC $d\hat{P}_n$ together with corresponding average values using training/testing dataset case E1 are shown and assuming absence of systematic errors because both meters were calibrated.

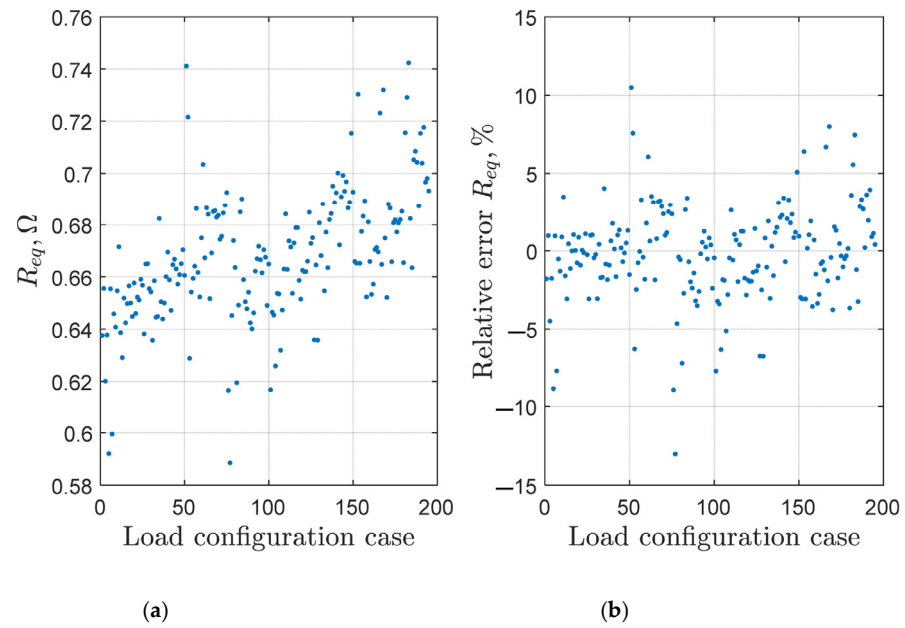


Figure 17. The equivalent resistance R_{eq} estimates (a) and relative error (b).

Table 8. Cases of training and testing measured datasets (total number of samples and percentage of the full dataset).

Dataset Case	Training Data Set	Testing Data Set
E1	98 samples/50% (odd samples, sample numbers $2n - 1$, n integer number from 1 to $N/2$)	97 samples/50% (even samples, sample numbers $2n$, n integer number from 1 to $N/2$)
E2	98 samples/50% (odd samples)	49 samples/25% (sample numbers $4n$, n integer number from 1 to $N/4$)
E3	98 samples/50% (odd samples)	25 samples/12.5% (sample numbers $8n$, n integer number from 1 to $N/8$)
E4	98 samples/50% (odd samples)	13 samples/6.25% (sample numbers $16n$, n integer number from 1 to $N/16$)

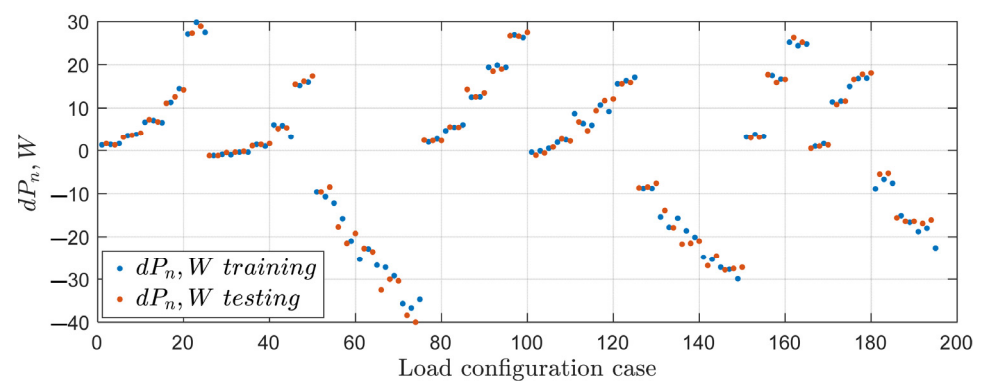


Figure 18. Measured dP_n samples split to 50% for training and 50% for testing datasets (E1 case).

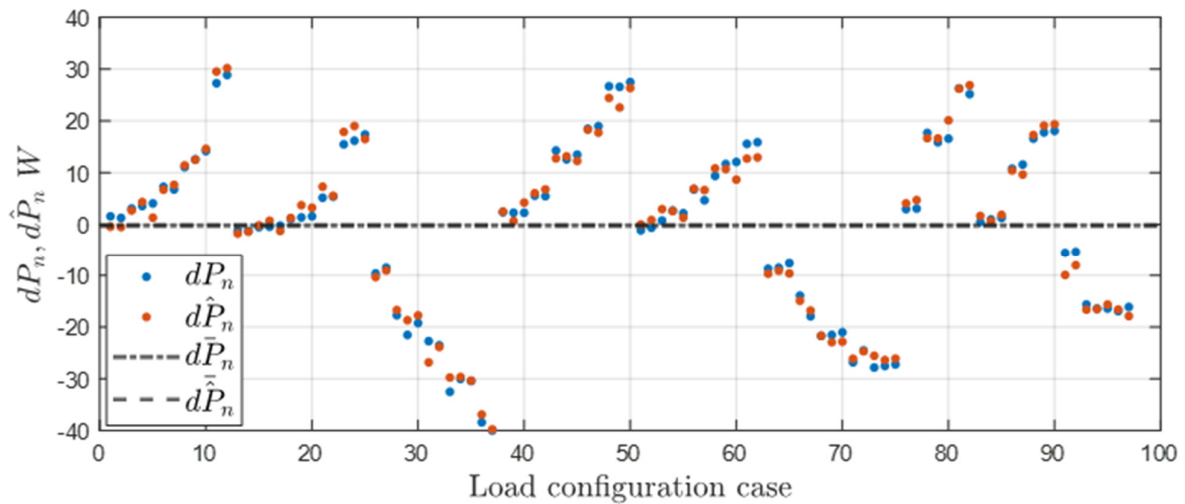


Figure 19. Measured PCC dP_n and prediction PCC $d\hat{P}_n$ (E1 case).

The difference between measured PCC dP_n and predicted PCC $d\hat{P}_n$ is in the range from -3.5 W to 4.4 W for the exercised testing data set E1 (Figure 20). Statistical parameters of $\overline{dP_n}$ are shown in Table 9 and include the difference between the average PCC obtained from measured PCC samples and the average of PCC estimates denoted as $\Delta(\overline{dP_n}) = \overline{dP_n} - \overline{d\hat{P}_n}$, the relative error of average PCC denoted as $e(\overline{dP_n}) = \Delta(\overline{dP_n}) / \overline{dP_n} \cdot 100\%$, and the standard deviation of all $\Delta(dP_n)$ samples (see Figure 20) denoted as $\sigma(\Delta(dP_n))$. The average values mentioned are always obtained from PCC samples measured of predicted using testing data set indicated in Table 9. Considering the power balance Equation (1), which can be averaged for multiple power events, parameters $\Delta(\overline{dP_n})$ and $\sigma(\Delta(dP_n))$ indicate how precisely the equality could be reached and how precisely meter gain errors estimated or other anomalies detected.

The relationship between the measured dP_n and the predicted $d\hat{P}_n$ is shown in Figure 21, indicating the quality of the built prediction model (26).

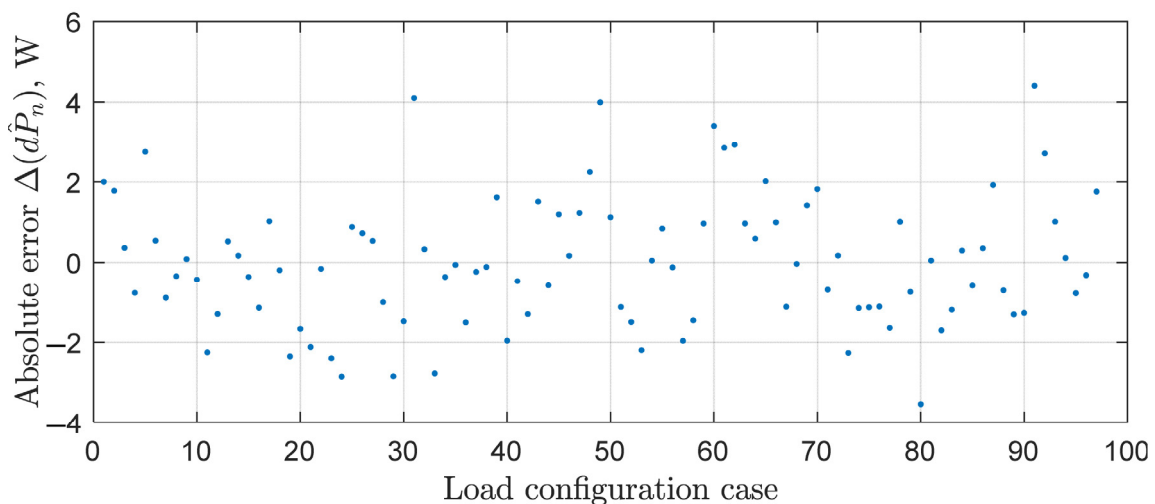
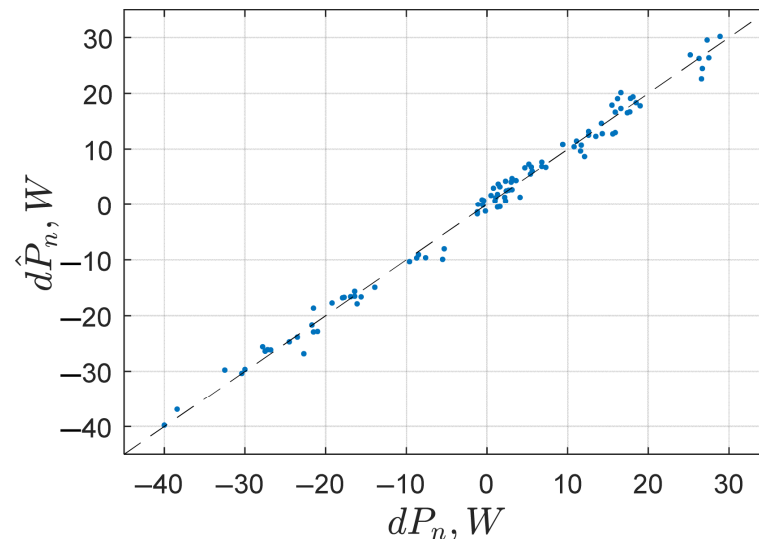


Figure 20. Prediction absolute error $\Delta(d\hat{P}_n)$ for dataset case E1.

Table 9. $\overline{dP_n}$ estimates and their statistical parameters.

Dataset Case	$\overline{dP_n}, W$	$\overline{d\hat{P}_n}, W$	$\Delta(\overline{dP_n}), W$	$e(\overline{dP_n}), \%$	$\sigma(\Delta(dP_n)), W$
E1	−0.17	−0.14	−0.03	13.53	1.64
E2	−1.26	−1.39	0.13	−10.41	1.83
E3	−1.11	−1.24	0.13	−11.22	1.92
E4	2.19	1.95	0.24	10.63	1.98

**Figure 21.** Scatterplot of dP_n prediction (dataset case E1, no systematic errors).

The influence of consumer MUT systematic error was examined by injecting $(\hat{e}_V, \hat{e}_P) = [(-2.5\%, -5\%), (-1.5\%, -3\%), (0\%, 0\%), (1.5\%, 3\%), (2.5\%, 5\%)]$ systematic errors to the testing data set samples and applying (24) to acquire estimates of these injected errors (\hat{e}_V, \hat{e}_P) as shown in Figure 22. The absolute error of estimation for testing datasets E1, E2, E3 is virtually equal to zero. This ideal situation can be justified by: (1) a very simple distribution grid branch equivalent schematics, which in opposite to real electrical grids, matches the assumed equivalent model for method equations development (Figure 4), (2) the limited search resolution when solving (24) using exhaustive search (0.1% for both e_V and e_P), and (3) the size and distribution of training data represented the full dataset very well, which enabled to build a data-driven model capable of high precision prediction (this could also be the case in real-life conditions when a consumer owns limited set of loads and operates them daily causing very similar power steps both at the period of model training and testing). It has to be emphasized, that the estimation error of power and voltage gain errors that are achievable in the range of 0.1% is quite sufficient for practical needs, for example, to decide about out-of-tolerance status of MUT. Yet another reason of very small error of estimation of gain error is probably lower level of random noise component in the readings of real smart meter utilized in the testbed compared to the random noise injected to the synthesized datasets used to estimate the performance of the PCC estimation method.

Despite the promising results of method performance using in-laboratory build test bed, the next step of testing in larger scale distribution network will be mandatory. For the setup upscaling a remote acquisition of electrical quantities readings has to be implemented maintaining a sufficient synchronization between sum meter and consumer MUT. The synchronization is expected to achieve using 1 s time stamps transmitted by smart meters over the external interface (P1 or Modbus). Data storage in the centralized database designed for experimental needs has to be created because utilities or external organizations

not always acquire and store all the readings which are available from smart meters and required for the implementation of the technique explored in this paper.

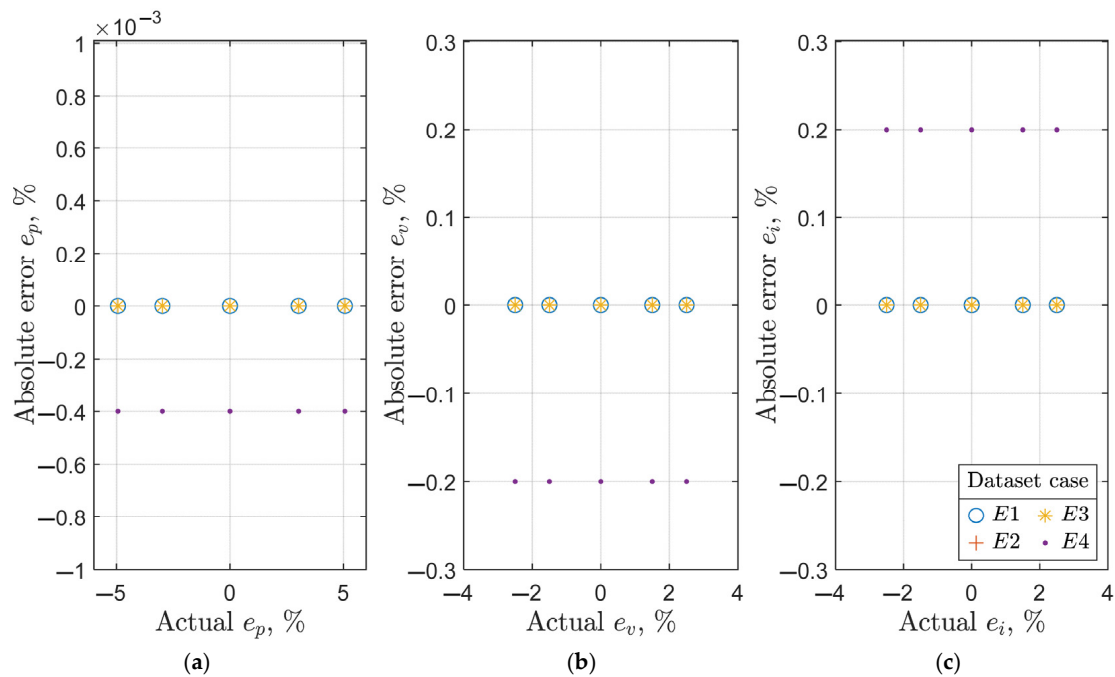


Figure 22. Absolute error of e_p (a), e_v (b), e_i (c) estimation for different testing dataset. Results of datasets E1, E2 and E3 are overlapped.

5. Discussion

The conducted analysis substantiates that PCC in a distributed grid (DG) branch, attributable to consumer load power event, is significantly influenced not only by the magnitude of the consumer power demand change but also by the characteristics of the other network loads—such as their ZIP model parameters—along with their sizes and location distribution across the grid. The lack of measurement data due to incomplete deployment of smart meters hinders accurate PCC estimation based solely on available readings. As a result, developing a predictive model to estimate PCC in response to power events becomes the only viable alternative.

The accuracy and robustness of such a model will depend strongly on the quality and quantity of data—including readings from sum and consumer meters—collected under controlled reference conditions and utilized for model training. A tradeoff is often sought between model complexity and the volume of training data to be collected and used during in-service grid and meter monitoring. This tradeoff is influenced by considerations such as anomaly or meter error detection speed (i.e., convergence rate) and the reliability of estimates (including meter error and PCC).

In case of a boundary option, one may rely on extended observation period during reference conditions and employ averaging techniques to derive model parameters that reflect the aggregate behavior of user loads, grid losses, and consumer activity. However, such a model does not capture the underlying physical phenomena of an electrical grid and require a large number of data samples to ensure reliable estimates of meter errors or PCC in the monitored distribution branch. In the extreme opposite case, it is feasible to construct data-driven models of higher complexity, capable of predicting the attributes of interest using less input (testing) data. Machine learning algorithms represent the most likely methodological choice and will be explored further in our subsequent research publications. Nonetheless, integrating fundamental principles of electrical grid physics into these models

may help overcome some of the inherent limitations of machine learning, which, being purely data-driven, necessitate extensive datasets encompassing diverse conditions and ranges of independent variables—a requirement that is not easily satisfied in real-world operational environments.

Although exploring advanced modeling techniques, including machine learning, for predicting $d\hat{P}_n$ is a promising direction, this task remains challenging due to the scarcity of voltage, current, and power data during consumer power event monitoring phases. Averaging $d\hat{P}_n$ might initially seem inappropriate given the variability in network configurations across different events, it remains valuable because the power balance Equation (1) retains validity when applied to averaged quantities. By averaging $d\hat{P}_n$ various grid and load setups are accounted for, thereby mitigating the impact of a single prediction error under some rear conditions, notwithstanding the loss of direct physical meaning.

Future scholarly work should focus on techniques for recognition of conditions for acquiring test data (including load setup, types, and locations) as compared to those during the data training phase. Additionally, aligning the consumer power steps recorded during monitoring with those from the model's training phase could enhance the repeatability of R_{eq} and dP_n estimates. Since the mean value of R_{eq} is used in monitoring phase, it is indeed important to acquire sufficient number of its samples (like 195 in Figure 17). Also, it has to be noted, that R_{eq} is the parameter of equivalent circuit and it is influenced by the mismatch between equivalent schematics (Figure 4) and electrical circuit used to generate training and testing datasets (Figure 1) or real electrical grid topology (in case of experimental testing in this article Figure 13). Therefore, the cause of samples dispersion is not only due to random measurement errors (outlier detection could reduce the dispersion of the mean estimate) of meters but also due to the power consumption and locations in the grid (Figure 4) and consumer power step size and consumption before the power step. Even though R_{eq} could be affected by these factors, it is the most important that its repeatability is ensured during testing compared to training phase. A way to reduce dispersion of mean value of R_{eq} is to seek for the similar conditions (same power steps, same initial consumer consumption, same total grid consumption) of R_{eq} sampling both during training and testing phases. Equivalent circuit parameter R_{eq} is aimed to model the distribution branch ohmic resistance, but it has to be non-sensitive to other mentioned power consumption conditions. The similar consideration for dP_n dispersion reduction applies.

The research must also continue in the aiming at method verification in real grid conditions. The key assumption of the event-driven technique [37] is that probability of power consumption changes of other consumers except the consumer whose load is metered by MUT is very low at the moment of power event (consumption change). Electrical quantities (voltage, current, power) before and after the power event are sampled during the time interval of 10 s before to 10 s after the moment of sudden power change. If at the same moment (in the period of 20 s) power events take place not only in the load of consumer monitored by MUT but at some other consumer loads, then the power balance equation definition (1) becomes not valid. Therefore, it is important that within this period (20 s) a consumption of other consumers remain constant, because their power consumption fluctuations influence readings of the sum meter. In case these rear events of overlapping of power consumption changes due to other consumers load activities, the data acquired at the moment of this power step must be rejected and not used for the PCC in the branch prediction or MUT gain error detection. Though not applied in this research (in synthesized data set and during experimental testing overlapping of power events was prevented), a quite simple rejection rules can be suggested, like if the difference between sum meter and consumer MUT power change differs more than a preset threshold, for example 10% (because typically power losses in LV distribution grid is less than 5%).

If power consumption before and after the power step is non-constant due to some power consumption transient processes or dynamic behavior, certain power step samples processing is applied as described in [37]. It is specified that the average of 10 samples (10 s) of $V/I/P$ before power step and average value of 10 samples (10 s) of $V/I/P$ after power step are used to calculate $V/I/P$ values before and after the power steps. Therefore, fluctuations of power $V/I/P$ are suppressed and their influence on dP , dV , and dI is minimized.

The influence of network noise did not deteriorate method performance during testing with experimental test bench, which was power from a LV network. A more extensive verification with sum meter placed at some network node closer to the transformer is underway and will be reported in follow-up research.

The influence of more specific energy quality indicators like voltage sags remains unexplored and should be targeted in the future. Nevertheless, we do not expect a severe influence because 10 voltage samples before and 10 samples after (sampling period is 1 s) will be always averaged and this should filter several periods voltage magnitude decrease during the sag. In case the sag continues for a longer period (minute), both sum meter and consumer MUT will sense the same voltage dip, and that will not be an issue for the method. Finally, some outlier rejection rules may be introduced if voltage sags cause distortions of meter readings and unexpectedly high PCC or meter gain error values.

To mention additional influencing factors for future analysis, it has to be noted that power losses in 3-phase distribution systems are influenced by the unbalance of load in different electrical phases [66,67]. At the moment of PCC, due to a single-phase load switching, the balancing conditions in the distribution grid are changing instantaneously. Consequently, the change of power losses measured by sum meter includes unbalanced conditions, caused power losses. Influence of phase load unbalance on power losses was investigated in [68,69], showing that it may contribute up to a $3.7 \div 6.4\%$ increase of power losses. Though such a size of losses seems comparable and even less than the error of PCC estimation by the presented method, it is important to investigate its influence in more detail in the future. Considering that instantaneous power consumption in all phases and in some implementations neutral current is available from a 3-phase sum meter, the unbalance factor before and after the power step could be obtained and used as inputs for dP_w and dP_{nL} correction. Implementation of the method in the existing monitoring systems may require some modifications to their current functionality. At this stage of development, this can be discussed only in a preliminary fashion. Some manufacturers of MDMS (Meter Data Management Systems) among the features list anomaly detection, but no more information is made open [70]. The deployment of various anomaly detection systems can either be based on readings accessible from smart meters. Siemens EnergyIP Mosaic, Landis+Gyr's Revelo are examples of AMI vendor-agnostic MDMS, promoting anomaly detection features. However, they are proprietary and not open for new developed techniques integration without vendor cooperation. Data storage and analytics could be integrated into (1) MDMS owned or operated by utilities or (2) operated by DSO-independent vendors. Though federated systems preserving user data privacy are discussed in scientific papers, the majority of methods described for anomaly detection are still based on centralized processing. In the application we consider in this paper a real-time detection is not mandatory. Indeed, it could last for weeks and months before a reliable detection of meter error is triggered. Every new application imposes certain requirements on the data collection system. Acquisition of electrical data from a smart meter at the rate of 1 s is commonly available over P1 interface. Therefore, technical solutions can rely on P1 local reading of measurements and delivering data to centralized processing servers. The amount of data to be transmitted over a communication channel (GSM, PLC, Wifi, etc.) and storage of data is a typical concern. An event-driven technique, as discussed in

this publication, requires high time resolution sampling (1 s) of electrical quantities, but only surrounding the moment of the power event. Therefore, detection of a power event should be implemented in the firmware of a smart meter and V/I/P samples 10 s before and after the power step delivered to the central server. At the same time, 20 s V/I/P readings from sum meter has to be requested and delivered to the same central server. Some implementation scenarios and load on the communication infrastructure have already been discussed in our previous publication [37].

6. Conclusions

A method has been developed to predict the power consumption change (PCC) in a distribution grid branch resulting from consumer load switching events. The predicted PCC enhances the accuracy of the active power balance equation, which is applied to the power readings from both the sum meter and the consumer smart meters at the moment of the consumer power demand change. By leveraging this improved power balance, the gain error in active power (or in voltage and current) measurements can be estimated, and other smart metering anomalies can be detected.

The total PCC in the distribution grid is decomposed into two components: one associated with distribution line losses and the other with consumers' load variations. The first component is approximated using an analytical expression based on an equivalent resistance value, estimated under reference conditions (i.e., during the training phase). The second component is approximated through a data-driven approach, which uses readings collected during these reference conditions from sum meter and consumer meter under test.

The accuracy of power gain error and PCC estimations is primarily influenced by the number of power events (and corresponding electrical measurements) used for model derivation and for the assessment of target values during the monitoring (testing) period. The improvement of accuracy class of the consumer meter from typical Class 1 to Class 0.5 was not found to have a noticeable influence on PCC prediction error, due to the statistical averaging of a sufficiently large number of events and other factors influencing accuracy of minimization problem solution necessary to obtain PCC estimate. Based on a synthesized dataset, the absolute error in estimating the power measurement gain error was within $\pm 0.3\%$, and the relative error in estimating the PCC in the distribution branch was within $\pm 10\%$. Both levels of precision are considered acceptable for practical applications, given that the objective of the methodology is not to replace formal metrological verification or laboratory calibration, but rather to enable anomaly detection in smart metering, which can trigger further investigation via regulated metrological procedures or consumer complaint handling mechanisms.

An experimental validation of the methodology was conducted using a laboratory testbed equipped with two commercial smart meters, confirming the suitability of the methodology for estimating measurement errors and assessing changes in power consumption in the grid segment between the sum and consumer meter. However, field tests in an actual distribution grid environment are still required to further validate the methodology under real-world operating conditions.

Author Contributions: Conceptualization, M.S., E.V. and Ž.N.; methodology, Ž.N.; software, M.S. and J.Š.; validation, M.S., J.Š., K.Z. and V.D.; investigation, E.V.; data curation, R.L. and V.D.; writing—original draft preparation, R.L., M.S. and J.Š.; writing—review and editing, Ž.N.; visualization, M.S. and J.Š.; funding acquisition, Ž.N. All authors have read and agreed to the published version of the manuscript.

Funding: This research was funded by Research Council of Lithuania (LMTLT), agreement No S-MIP-24-42.

Institutional Review Board Statement: Not applicable.

Informed Consent Statement: Not applicable.

Data Availability Statement: The original data presented in the study are openly available at https://github.com/KTU-ANODETEL/Grid_of_6_Nodes_One_Phase_Dataset1, accessed on 14 June 2025.

Conflicts of Interest: The authors declare no conflicts of interest.

Abbreviations

AMI	Advanced Metering Infrastructure
DG	Distribution Grid Branch
DL	Distribution lines
DSMR	The Dutch standard for smart metering (NTA 8130)
E1	Experimental training and testing case 1
E2	Experimental training and testing case 2
E3	Experimental training and testing case 3
E4	Experimental training and testing case 4
K1–K5	Relays
LV	Low voltage (230/400 V)
M1	Meter class and random power error case 1
M2	Meter class and random power error case 2
M3	Meter class and random power error case 3
MDMS	Meter Data Management System
MUT	Meter under test
MV	Medium voltage (typically 10–20 kV)
OM	Ohmmeter
P1	Port of smart electricity meters
PCC	Power consumption change
PLC	Power Line Carrier
P_{L1}, P_{L2}	Loads
RB	Relay control block
RMSE	Root mean squared error
RS-232	A hardware standard for asynchronous serial communication
T1	Training data/Testing data case 1
T2	Training data/Testing data case 2
T3	Training data/Testing data case 3
USB	Universal Serial Bus
ZIP	A load model used in power system analysis to represent how the power consumption of a load changes with voltage. It combines three load characteristics: constant impedance (ZZ), constant current (ZI), and constant power (ZP)
Variables	
dI_s	The change of sum meter current (A)
dP_A	The PCC associated with a presence of the anomaly (W)
dP_c	An active PCC of the load located under the consumer MUT (W)

dP_i	PCC component of a particular load (W)
dP_{Li}	The PCC of network loads (W)
dP_n	The change of active powers in the network (W)
$\overline{dP_n}$	Mean value of real values dP_n (W)
$d\hat{P}_n$	Predicted change of active powers in the network (W)
$\overline{d\hat{P}_n}$	Mean value of predicted values $d\hat{P}_n$ (W)
dP_{nL}	The PCC associated with the grid and power of the grid loads (W)
$d\hat{P}_{nL}$	Predicted dP_{nL} (W)
dP_{Rs}	The PCC of consumption within the R_s branch (W)
dP_s	An active power change at the sum meter installation point (W)
$d\hat{P}_s$	Predicted active PCC at the sum meter installation point (W)
dP_w	The PCC associated with a technical power loss (W)
$d\hat{P}_w$	Predicted PCC associated with a technical power loss (W)
dP_{wi}	The PCC of consumption within the i th energy delivery branch (W)
dV_c	The change of consumer meter voltage (V)
dV_s	The change of sum meter voltage (V)
E_I	The relative percentage gain errors of current (%)
E_V	The relative percentage gain errors of voltage (%)
$e(\overline{d\hat{P}_n})$	Relative error of $d\hat{P}_n$ (%)
e_I	Systematic components of relative percentage gain errors of current (%)
\hat{e}_I	Predicted systematic components of relative percentage gain errors of current (%)
e_P	Systematic components of relative percentage gain errors of power (%)
\hat{e}_P	Predicted systematic components of relative percentage gain errors of power (%)
$e(R_{eq})$	Relative error of R_{eq} (%)
e_V	Systematic components of relative percentage gain errors of voltage (%)
\hat{e}_V	Predicted systematic components of relative percentage gain errors of voltage (%)
$e(\sigma(\Delta(d\hat{P}_n)))$	Relative error of the standard deviation $\sigma(\Delta(d\hat{P}_n))$ of absolute error $\Delta(d\hat{P}_n)$ values (%)
I	Current with added error (A)
I_0	Error-free values of the current obtained during synthesis (A)
I_{c1}	Consumer meter current before power step dP_c with random noise and systematic gain errors, and resolution (A)
I_{c2}	Consumer meter current after power step dP_c with random noise and systematic gain errors, and resolution (A)
I_{read}	The current reading displayed with resolution (A)
I_{s1}	Sum meter current before power step dP_c with random noise and resolution (A)
I_{s2}	Sum meter current after power step dP_c with random noise and resolution (A)
I_{wi1}	The currents in the i th line (cable) segment, correspondingly, before power step dP_c (A)
I_{wi2}	The currents in the i th line (cable) segment, correspondingly, after power step dP_c (A)
K	It is set to 10. Number for averaging of measurements.
N	Number of line segments between consecutive load connection points in the grid
P	Power with added error (W)
P_c	Consumer meter power (W)
P_{c1}	Consumer meter power before power step dP_c with random noise and systematic gain errors, and resolution (W)
P_{c2}	Consumer meter power after power step dP_c with random noise and systematic gain errors, and resolution (W)

P_{eqn}	The aggregate power consumption of the DG branch (W)
P_{iN}	Power consumed by i th load when its voltage equals to the nominal (W)
P_{Li}	Network active loads power (W)
P_{Rs}	The power consumption within the R_s branch (W)
P_{s1}	Sum meter power before power step dP_c with random noise and resolution (W)
P_{s2}	Sum meter power after power step dP_c with random noise and resolution (W)
P_{wi}	The power consumption within the i th energy delivery branch (W)
R_{eq}	The equivalent resistance (Ω)
$\overline{R_{eq}}$	Mean value of the equivalent resistance (Ω)
R_s	Wire resistance between sum meter and first line's (cable's) segment (Ω)
R_T	Wire resistance between transformer and sum meter (Ω)
R_{wi}	Wire resistance of the i th line's (cable's) segment (Ω)
R_{wsum}	Sum of wire resistances of the i th line's (cable's) segment between sum meter and consumer meter (Ω)
res	Resolution of the current reading
r_I	Random components of relative percentage gain errors of current (%)
r_P	Random components of relative percentage gain errors of power (%)
r_V	Random components of relative percentage gain errors of voltage (%)
S_{IV}	The minimization task
V	Voltage with added error (V)
V_0	Error-free values of the voltage obtained during synthesis (V)
V_{c1}	Consumer meter voltage before power step dP_c with random noise and systematic gain errors, and resolution (V)
V_{c2}	Consumer meter voltage after power step dP_c with random noise and systematic gain errors, and resolution (V)
V_i	Nominal voltage (V)
V_{i1}	Actual voltages of the nodes where i th load is connected, correspondingly, before power step dP_c (V)
V_{i2}	Actual voltages of the nodes where i th load is connected, correspondingly, after power step dP_c (V)
V_N, a_i, b_i, c_i	The coefficients representing the constant power, constant current, and constant impedance components of the ZIP load model
V_{s1}	Sum meter voltage before power step dP_c with random noise and resolution (V)
V_{s2}	Sum meter voltage after power step dP_c with random noise and resolution (V)
γ_I	Relative systematic gain error of current
$\hat{\gamma}_I$	Predicted relative systematic gain error of current
γ_V	Relative systematic gain error of voltage
$\hat{\gamma}_P$	Predicted relative systematic gain error of power
$\hat{\gamma}_V$	Predicted relative systematic gain error of voltage
$\Delta(\overline{dP_n})$	The absolute error between predicted and real $\overline{dP_n}$ (W)
$\Delta(d\hat{P}_n)$	The absolute error between predicted and real dP_n (W)
$\Delta(dP_{nL})$	The absolute error between predicted and real dP_{nL} (W)
$\Delta(e_V)$	Estimation error of the systematic gain error for voltage (%)
δ_I	Relative random gain error of current
δ_V	Relative random gain error of voltage
$\sigma(e(\overline{R_{eq}}))$	The standard deviation of estimation error mean of R_{eq} (%)
$\sigma(\overline{\Delta(e_V)})$	Standard deviation of mean of estimation error of the systematic gain error for voltage (%)
$\sigma(\Delta(dP_n))$	Standard deviation of absolute error of dP_n (W)

References

1. Molina-Solana, M.; Ros, M.; Dolores Ruiz, M.; Gómez-Romero, J.; Martín-Bautista, M.J. Data science for building energy management: A review. *Renew. Sustain. Energy Rev.* **2017**, *70*, 598–609. [\[CrossRef\]](#)
2. Rind, Y.M.; Raza, M.H.; Zubair, M.; Mehmood, M.Q.; Massoud, Y. Smart Energy Meters for Smart Grids, an Internet of Things Perspective. *Energies* **2023**, *16*, 1974. [\[CrossRef\]](#)
3. Shafique, H.; Bertling Tjernberg, L.; Archer, D.-E.; Wingstedt, S. Behind the Meter Strategies: Energy management system with a Swedish case study. *IEEE Electr. Mag.* **2021**, *9*, 112–119. [\[CrossRef\]](#)
4. Knayer, T.; Kryvinska, N. An analysis of smart meter technologies for efficient energy management in households and organizations. *Energy Rep.* **2022**, *8*, 4022–4040. [\[CrossRef\]](#)
5. Koukouvinos, K.G.; Koukouvinos, G.K.; Chalkiadakis, P.; Kaminaris, S.D.; Orfanos, V.A.; Rimpas, D. Evaluating the Performance of Smart Meters: Insights into Energy Management, Dynamic Pricing and Consumer Behavior. *Appl. Sci.* **2025**, *15*, 960. [\[CrossRef\]](#)
6. Avancini, D.B.; Rodrigues, J.J.P.C.; Martins, S.G.B.; Rabêlo, R.A.L.; Al-Muhtadi, J.; Solic, P. Energy meters evolution in smart grids: A review. *J. Clean. Prod.* **2019**, *217*, 702–715. [\[CrossRef\]](#)
7. Avancini, D.B.; Rodrigues, J.J.P.C.; Rabêlo, R.A.L.; Das, A.K.; Kozlov, S.; Solic, P. A new IoT-based smart energy meter for smart grids. *Int. J. Energy Res.* **2021**, *45*, 189–202. [\[CrossRef\]](#)
8. Sun, Q.; Li, H.; Ma, Z.; Wang, C.; Campillo, J.; Zhang, Q.; Wallin, F.; Guo, J. A Comprehensive Review of Smart Energy Meters in Intelligent Energy Networks. *IEEE Internet Things J.* **2016**, *3*, 464–479. [\[CrossRef\]](#)
9. Kilius, Š.; Gailius, D.; Knyva, M.; Balčiūnas, G.; Meškuotienė, A.; Dobilienė, J.; Joneliūnas, S.; Kuzas, P. Time Delay Characterization in Wireless Sensor Networks for Distributed Measurement Applications. *J. Sens. Actuator Netw.* **2024**, *13*, 31. [\[CrossRef\]](#)
10. Raza, M.H.; Rind, Y.M.; Javed, I.; Zubair, M.; Mehmood, M.Q.; Massoud, Y. Smart Meters for Smart Energy: A Review of Business Intelligence Applications. *IEEE Access* **2023**, *11*, 120001–120022. [\[CrossRef\]](#)
11. Liu, X.; Nielsen, P.S. Scalable prediction-based online anomaly detection for smart meter data. *Inf. Syst.* **2018**, *77*, 34–47. [\[CrossRef\]](#)
12. Yip, S.C.; Wong, K.S.; Hew, W.P.; Gan, M.T.; Phan, R.C.W.; Tan, S.W. Detection of energy theft and defective smart meters in smart grids using linear regression. *Int. J. Electr. Power Energy Syst.* **2017**, *91*, 230–240. [\[CrossRef\]](#)
13. Nakutis, Ž.; Kaškonas, P. A Contemplation on Electricity Meters In-Service Surveillance Assisted by Remote Error Monitoring. *Energies* **2020**, *13*, 5245. [\[CrossRef\]](#)
14. Sun, Y.; Sun, X.; Hu, T.; Zhu, L. Smart Grid Theft Detection Based on Hybrid Multi-Time Scale Neural Network. *Appl. Sci.* **2023**, *13*, 5710. [\[CrossRef\]](#)
15. Zhang, L.; Wan, L.; Xiao, Y.; Li, S.; Zhu, C. Anomaly Detection method of Smart Meters data based on GMM-LDA clustering feature Learning and PSO Support Vector Machine. In Proceedings of the 2019 IEEE Sustainable Power and Energy Conference (iSPEC), Beijing, China, 21–23 November 2019; pp. 2407–2412. [\[CrossRef\]](#)
16. Kim, J.Y.; Hwang, Y.M.; Sun, Y.G.; Sim, I.; Kim, D.I.; Wang, X. Detection for Non-Technical Loss by Smart Energy Theft with Intermediate Monitor Meter in Smart Grid. *IEEE Access* **2019**, *7*, 129043–129053. [\[CrossRef\]](#)
17. Moghaddass, R.; Wang, J. A Hierarchical Framework for Smart Grid Anomaly Detection Using Large-Scale Smart Meter Data. *IEEE Trans. Smart Grid* **2018**, *9*, 5820–5830. [\[CrossRef\]](#)
18. Utomo, D.; Hsiung, P.-A. A Multitiered Solution for Anomaly Detection in Edge Computing for Smart Meters. *Sensors* **2020**, *20*, 5159. [\[CrossRef\]](#)
19. Jithish, J.; Alangot, B.; Mahalingam, N.; Yeo, K.S. Distributed Anomaly Detection in Smart Grids: A Federated Learning-Based Approach. *IEEE Access* **2023**, *11*, 7157–7179. [\[CrossRef\]](#)
20. Liu, F.; Huang, H. Smart Meter Error Estimation in Topological Low Voltage Energy System. *IEEE Access* **2024**, *12*, 147422–147437. [\[CrossRef\]](#)
21. Kong, X.; Ma, Y.; Zhao, X.; Li, Y.; Teng, Y. A Recursive Least Squares Method with Double-Parameter for Online Estimation of Electric Meter Errors. *Energies* **2019**, *12*, 805. [\[CrossRef\]](#)
22. Duan, J.; Tang, Q.; Ma, J.; Yao, W. Operational Status Evaluation of Smart Electricity Meters Using Gaussian Process Regression with Optimized-ARD Kernel. *IEEE Trans. Ind. Inform.* **2024**, *20*, 1272–1282. [\[CrossRef\]](#)
23. Liu, Y.; Zhao, Q.; Liang, D.; Han, Y.; Zhang, Y.; Guo, H. Research on Operation Error Detection Model of Metering Device. In Proceedings of the 2023 IEEE/IAS Industrial and Commercial Power System Asia (I&CPS Asia), Chongqing, China, 7–9 July 2023; pp. 232–237. [\[CrossRef\]](#)
24. Helong, L.; Haibo, Y.; Jinshuai, Y. Intelligent Energy Meter Fault Prediction Based on Machine Learning. In Proceedings of the 2019 15th International Conference on Computational Intelligence and Security (CIS), Macao, China, 13–16 December 2019; pp. 296–300. [\[CrossRef\]](#)
25. Zhao, Z.; Chen, Y.; Liu, J.; Cheng, Y.; Tang, C.; Yao, C. Evaluation of Operating State for Smart Electricity Meters Based on Transformer–Encoder–BiLSTM. *IEEE Trans. Ind. Inform.* **2023**, *19*, 2409–2420. [\[CrossRef\]](#)

26. Feng, Z.; Yingying, C.; Jie, D.; Ling, F.; Ji, X.; Jiaming, Z.; Huayong, Z. Construction of Multidimensional Electric Energy Meter Abnormal Diagnosis Model Based on Decision Tree Group. In Proceedings of the 2019 IEEE 8th Joint International Information Technology and Artificial Intelligence Conference (ITAIC), Chongqing, China, 24–26 May 2019; pp. 1687–1691. [\[CrossRef\]](#)
27. He, C.; Xia, X.; Zhang, B.; Kang, W.; Zhang, J.; Chen, H. Analyzing adjustment and verification errors in electric metering devices for smart power systems considering multiple environmental factors. *AIP Adv.* **2024**, *14*, 125319. [\[CrossRef\]](#)
28. Nakutis, Ž.; Kaškonas, P.; Saunoris, M.; Daunoras, V.; Jurčević, M. A framework for remote in-service metrological surveillance of energy meters. *Measurement* **2021**, *168*, 108438. [\[CrossRef\]](#)
29. Civelek, O.; Gormus, S.; Okumus, H.I.; Yilmaz, H. Combating electricity theft in smart grids: Accurate location identification using machine learning and the fast Walsh–Hadamard transform. *Electr. Eng.* **2024**, *107*, 6165–6179. [\[CrossRef\]](#)
30. Bondok, A.; Abdelsalam, O.; Badr, M.; Mahmoud, M.; Alsabaan, M.; Alsaqhan, M.; Ibrahim, M.I. Accurate Power Consumption Predictor and One-Class Electricity Theft Detector for Smart Grid “Change-and-Transmit” Advanced Metering Infrastructure. *Appl. Sci.* **2024**, *14*, 9308. [\[CrossRef\]](#)
31. Bonci, A.; Fredianelli, L.; Kermenov, R.; Longarini, L.; Longhi, S.; Pompei, G.; Prist, M.; Verdini, C. DeepESN Neural Networks for Industrial Predictive Maintenance through Anomaly Detection from Production Energy Data. *Appl. Sci.* **2024**, *14*, 8686. [\[CrossRef\]](#)
32. Oprea, S.-V.; Bâra, A.; Puican, F.C.; Radu, I.C. Anomaly Detection with Machine Learning Algorithms and Big Data in Electricity Consumption. *Sustainability* **2021**, *13*, 10963. [\[CrossRef\]](#)
33. Pereira, J.; Silveira, M. Unsupervised Anomaly Detection in Energy Time Series Data Using Variational Recurrent Autoencoders with Attention. In Proceedings of the 2018 17th IEEE International Conference on Machine Learning and Applications (ICMLA), Orlando, FL, USA, 17–20 December 2018. [\[CrossRef\]](#)
34. Žarković, M.; Dobrić, G. Artificial Intelligence for Energy Theft Detection in Distribution Networks. *Energies* **2024**, *17*, 1580. [\[CrossRef\]](#)
35. Korhonen, A. Verification of Energy Meters Using Automatic Meter Reading Data. Master’s Thesis, School of Electrical Engineering, Aalto University, Espoo, Finland, 2012.
36. Fangxing, L.; Chengbin, L.; Qing, H. A Data-Based Approach for Smart Meter Online Calibration. *Acta IMEKO* **2020**, *9*, 32–37. [\[CrossRef\]](#)
37. Nakutis, Ž.; Rinaldi, S.; Kuzas, P.; Lukočius, R. A Method for Noninvasive Remote Monitoring of Energy Meter Error Using Power Consumption Profile. *IEEE Trans. Instrum. Meas.* **2020**, *69*, 6677–6685. [\[CrossRef\]](#)
38. Raesaar, P.; Tiigimägi, E.; Valtin, J. Strategy for analysis of loss situation and identification of loss sources in electricity distribution networks. *Oil Shale* **2007**, *24*, 297–307. [\[CrossRef\]](#)
39. Poursharif, G.; Brint, A.; Black, M.; Marshall, M. Using smart meters to estimate low-voltage losses. *IET Gener. Transm. Distrib.* **2018**, *12*, 1206–1212. [\[CrossRef\]](#)
40. Pilo, F.; Bertani, A.; Celli, G.; Tardio, M.; Soma, G.G.; Pannunzio, G. Technical Losses Assessment in Distribution Systems with Reduced Measurement Capabilities. In Proceedings of the 23rd International Conference on Electricity Distribution, Lyon, France, 15–18 June 2015.
41. Lawanson, T.; Ravikumar, K.; Schulz, D.; Cecchi, V. Loss Estimation and Visualization in Distribution Systems using Smart Meter and Recloser Data. In Proceedings of the 2019 IEEE 16th International Conference on Smart Cities: Improving Quality of Life Using ICT & IoT and AI (HONET-ICT), Charlotte, NC, USA, 6–9 October 2019. [\[CrossRef\]](#)
42. Rendroyoko, I.; Nungtjik, I.; Suhana, H.H. Development of Large Scale, End-to-End Online Monitoring Losses (OML). In Proceedings of the 2022 5th International Conference on Power Engineering and Renewable Energy (ICPERE), Bandung, Indonesia, 22–23 November 2022. [\[CrossRef\]](#)
43. Nainar, K.; Iov, F. Three-Phase State Estimation for Distribution-Grid Analytics. *Clean Technol.* **2021**, *3*, 395–408. [\[CrossRef\]](#)
44. Velasco, J.A.; Amaris, H.; Alonso, M.; Miguelez, M. Stochastic Technical Losses Analysis of Smart Grids under Uncertain Demand. In Proceedings of the 2018 53rd International Universities Power Engineering Conference (UPEC), Glasgow, UK, 4–7 September 2018. [\[CrossRef\]](#)
45. Velasco, J.A.; Amaris, H.; Alonso, M.; Casas, M. Energy losses estimation tool for Low Voltage Smart grids. In Proceedings of the CIRED Conference-25th International Conference on Electricity Distribution, Madrid, Spain, 3–6 June 2019.
46. Li, Z.; Sun, H.; Xue, Y.; Li, Z.; Jin, X.; Wang, P. Resilience-Oriented Asynchronous Decentralized Restoration Considering Building and E-Bus Co-Response in Electricity-Transportation Networks. *IEEE Trans. Transp. Electr.* **2025**; early access. [\[CrossRef\]](#)
47. Telford, R.; Stephen, B.; Browell, J.; Haben, S. Dirichlet Sampled Capacity and Loss Estimation for LV Distribution Networks with Partial Observability. *IEEE Trans. Power Deliv.* **2021**, *36*, 2676–2686. [\[CrossRef\]](#)
48. Velasco, J.A.; Amaris, H.; Alonso, M. Deep Learning loss model for large-scale low voltage smart grids. *Int. J. Electr. Power Energy Syst.* **2020**, *121*, 106054. [\[CrossRef\]](#)
49. Au, M.T.; Anthony, T.M.; Kamaruddin, N.; Verayiah, R.; Syed Mustaffa, S.A.; Yusoff, M. A simplified approach in estimating technical losses in distribution network based on load profile and feeder characteristics. In Proceedings of the 2008 IEEE 2nd International Power and Energy Conference, Johor Bahru, Malaysia, 1–3 December 2008. [\[CrossRef\]](#)

50. Queiroz, L.M.O.; Roselli, M.A.; Cavellucci, C.; Lyra, C. Energy Losses Estimation in Power Distribution Systems. *IEEE Trans. Power Syst.* **2012**, *27*, 1879–1887. [\[CrossRef\]](#)
51. Oliveira, M.E.; Padilha-Feltrin, A. A Top-Down Approach for Distribution Loss Evaluation. *IEEE Trans. Power Deliv.* **2009**, *24*, 2117–2124. [\[CrossRef\]](#)
52. Fu, X.; Chen, H.; Cai, R.; Xuan, P. Improved Isf method for loss estimation and its application in dg allocation. *IET Gener. Transm. Distrib.* **2016**, *10*, 2512–2519. [\[CrossRef\]](#)
53. Mazza, A.; Chicco, G. High-Quality Load Pattern Reconstruction from Smart Meter Data to Enhance the Assessment of Peak Power and Network Losses. *IEEE Trans. Ind. Appl.* **2022**, *58*, 3261–3274. [\[CrossRef\]](#)
54. Chenjie, M.; Menke, J.-H.; Dasenbrock, J.; Braun, M.; Haslbeck, M.; Schmid, K.-H. Evaluation of energy losses in low voltage distribution grids with high penetration of distributed generation. *Appl. Energy* **2019**, *256*, 113907. [\[CrossRef\]](#)
55. Zhu, W.; Zhou, Q.; An, H.; Chen, Z.; Liu, S.; Yu, K. Analysis of the correlation between characteristic of equivalent load and power loss in smart distribution grid. In Proceedings of the 2017 2nd International Conference on Power and Renewable Energy (ICPRE), Chengdu, China, 20–23 September 2017. [\[CrossRef\]](#)
56. Wang, S.; Dong, P.; Tian, Y. A Novel Method of Statistical Line Loss Estimation for Distribution Feeders Based on Feeder Cluster and Modified XGBoost. *Energies* **2017**, *10*, 2067. [\[CrossRef\]](#)
57. Wang, B.; Sun, Y.; Lu, F.; Wu, X. The Calculation and Analysis of Distribution Network Loss with Photovoltaic Power Generation Connected. In Proceedings of the 3rd International Conference on Advances in Energy and Environmental Science 2015, Zhuhai, China, 25–26 July 2015. [\[CrossRef\]](#)
58. Ibrahim, K.A.; Au, M.T.; Gan, C.K.; Tang, J.H. System wide MV distribution network technical losses estimation based on reference feeder and energy flow model. *Int. J. Electr. Power Energy Syst.* **2017**, *93*, 440–450. [\[CrossRef\]](#)
59. Dashtaki, A.K.; Haghifam, M.R. A new loss estimation method in limited data electric distribution network. *IEEE Trans. Power Deliv.* **2013**, *28*, 2194–2200. [\[CrossRef\]](#)
60. Grigoras, G.; Neagu, B.-C. Smart Meter Data-Based Three-Stage Algorithm to Calculate Power and Energy Losses in Low Voltage Distribution Networks. *Energies* **2019**, *12*, 3008. [\[CrossRef\]](#)
61. Soares, T.M.; Bezerra, U.H.; Tostes, M.E.D.L. Full-Observable Three-Phase State Estimation Algorithm Applied to Electric Distribution Grids. *Energies* **2019**, *12*, 1327. [\[CrossRef\]](#)
62. Kłosowski, Z.; Mazur, Ł. Influence of the Type of Receiver on Electrical Energy Losses in Power Grids. *Energies* **2023**, *16*, 5660. [\[CrossRef\]](#)
63. Diahovchenko, I.; Petrichenko, L. Assessment of energy losses in power distribution systems with individual prosumers and energy communities. *J. Eng.* **2023**, *2023*, e12243. [\[CrossRef\]](#)
64. Henriques, H.O.; Corrêa, R.L.S.; Fortes, M.Z.; Borba, B.S.M.C.; Ferreira, V.H. Monitoring technical losses to improve non-technical losses estimation and detection in LV distribution systems. *Measurement* **2020**, *161*, 107840. [\[CrossRef\]](#)
65. Jayasinghe, H.; Gunawardane, K.; Nicholson, R. Applications of Electrical Load Modelling in Digital Twins of Power Systems. *Energies* **2025**, *18*, 775. [\[CrossRef\]](#)
66. Tavakoli Bina, M.; Kashefi, A. Three-phase unbalance of distribution systems: Complementary analysis and experimental case study. *Int. J. Electr. Power Energy Syst.* **2011**, *33*, 817–826. [\[CrossRef\]](#)
67. Shen, Z.; Zheng, Z.; Fu, Y.; Yin, Z. The Impact of Three-phase Unbalance in Power Grid on the Losses of Distribution Equipment. In Proceedings of the 2nd International Conference on Smart Grids and Energy Systems 2023, Guangzhou, China, 25–27 August 2023; pp. 106–109. [\[CrossRef\]](#)
68. Ochoa, L.F.; Ciric, R.M.; Padilha-Feltrin, A.; Harrison, G.P. Evaluation of distribution system losses due to load unbalance. In Proceedings of the 15th Power Systems Computation Conference PSCC 2005, Liège, Belgium, 22–26 August 2005; pp. 1–4.
69. Dong, Y. Research on Loss in Power Grid Induced by Three-Phase Imbalance. *J. Electr. Electron. Eng.* **2020**, *8*, 103–108. [\[CrossRef\]](#)
70. Jones, L.; Sumi, Z. *Market Guide for Meter Data Management Systems*; Gartner Research: Stamford, CT, USA, 24 January 2023; Available online: <https://www.gartner.com/en/documents/4023263> (accessed on 2 June 2025).

Disclaimer/Publisher’s Note: The statements, opinions and data contained in all publications are solely those of the individual author(s) and contributor(s) and not of MDPI and/or the editor(s). MDPI and/or the editor(s) disclaim responsibility for any injury to people or property resulting from any ideas, methods, instructions or products referred to in the content.